Stratospheric chlorine processing after the unprecedented Hunga Tonga eruption

Jun Zhang[1], Peidong Wang[2], Douglas Edward Kinnison[3], Susan Solomon[4], Jian Guan[2], and Yunqian Zhu[5]

[1]NSF National Center for Atmospheric Research
[2]Massachusetts Institute of Technology
[3]NCAR/CLAS
[4]MIT
[5]University of Colorado Boulder

February 16, 2024

Abstract

Following the Hunga Tonga–Hunga Ha'apai (HTHH) eruption in January 2022, a significant reduction in stratospheric hydrochloric acid (HCl) was observed in the Southern Hemisphere mid-latitudes during the latter half of 2022, suggesting potential chlorine activation. The objective of this study is to comprehensively understand the substantial loss of HCl in the aftermath of HTHH. Satellite measurements along with a global chemistry-climate model are employed for the analysis. We find strong agreement of 2022 anomalies between the modeled and the measured data. The observed tracer-tracer relations between N2O and HCl indicate a significant role of chemical processing in the observed HCl reduction, especially during the austral winter of 2022. Further examining the roles of chlorine gas-phase and heterogeneous chemistry, we find that heterogeneous chemistry emerges as the primary driver for the chemical loss of HCl, with the reaction between HOBr and HCl on sulfate aerosols identified as the dominant loss process.

Stratospheric chlorine processing after the unprecedented Hunga Tonga eruption

Authors: Jun Zhang[1*], Peidong Wang[2], Douglas Kinnison[1], Susan Solomon[2], Jian Guan[2], Yunqian Zhu[3,4]

Affiliations:

[1]Atmospheric Chemistry Observations & Modeling Laboratory, NSF National Center for Atmospheric Research, Boulder, CO, USA

[2] Department of Earth, Atmospheric, and Planetary Sciences, Massachusetts Institute of Technology, Cambridge, MA, USA, 02139

[3] Cooperative Institute for Research in Environmental Sciences, University of Colorado Boulder, Boulder, CO, USA, 80309

[4]Chemical Sciences Laboratory, National Oceanic and Atmospheric Administration, Boulder, CO, USA, 80305

[*]Corresponding author: Jun Zhang (jzhan166@ucar.edu)

Key Points:

- A significant reduction in stratospheric HCl was observed in the Southern Hemisphere mid-latitudes during the latter half of 2022.
- Analysis using both model and satellites suggest a significant role of chemical processing in the observed HCl reduction.
- Heterogeneous chemistry is the primary driver for the chemical HCl loss, with HOBr + HCl on sulfate aerosols as the dominant process.

Abstract

Following the Hunga Tonga–Hunga Ha'apai (HTHH) eruption in January 2022, a significant reduction in stratospheric hydrochloric acid (HCl) was observed in the Southern Hemisphere mid-latitudes during the latter half of 2022, suggesting potential chlorine activation. The objective of this study is to comprehensively understand the substantial loss of HCl in the aftermath of HTHH. Satellite measurements along with a global chemistry-climate model are employed for the analysis. We find strong agreement of 2022 anomalies between the modeled and the measured data. The observed tracer-tracer relations between N_2O and HCl indicate a significant role of chemical processing in the observed HCl reduction, especially during the austral winter of 2022. Further examining the roles of chlorine gas-phase and heterogeneous chemistry, we find that heterogeneous chemistry emerges as the primary driver for the chemical loss of HCl, with the reaction between HOBr and HCl on sulfate aerosols identified as the dominant loss process.

Plain language summary

After the eruption of Hunga Tonga–Hunga Ha'apai (HTHH) in January 2022, there was a substantial decrease in stratospheric hydrochloric acid (HCl) in the Southern Hemisphere mid-latitudes in the latter part of 2022, hinting at potential chlorine activation. This study aims to comprehensively understand the significant loss of HCl following the HTHH eruption, utilizing satellite measurements and a global chemistry-climate model for analysis. The anomalies in 2022 show remarkable agreement between the modeled and measured data. Tracer-tracer relations between N_2O and HCl suggest a substantial influence of chemical processing in the observed reduction of HCl, particularly during the austral winter of 2022. Upon further investigation into the role of chlorine gas-phase and heterogeneous chemistry, heterogeneous chemistry emerges as the primary driver for the chemical loss of HCl. The reaction between HOBr and HCl on sulfate aerosols is identified as the dominant process leading to this loss.

1. Introduction

The January 2022 Hunga Tonga–Hunga Ha'apai (HTHH) eruption (20.5°S, 175.4°W) was an unprecedented underwater volcanic event in the modern era. The eruption injected about 150 Tg of water (H_2O) (Millán et al., 2022; Randel et al., 2023) along with a moderate amount of sulfur dioxide (SO_2) into the stratosphere (Carn et al. 2022; Taha et al., 2022). Satellite observations (Santee et al., 2023) and model simulations (Zhang et al., 2023; Wilmouth et al., 2023), all found significant ozone decreases in the lower stratosphere at southern hemisphere (SH) mid-latitudes in 2022 after the eruption. In particular, a record low ozone relative to the climatology (2004 to 2021) in the SH austral winter between 30 to 50 hPa was observed in the mid-latitudes (Zhang et al., 2023). While there is evidence for some dynamical contributions to the ozone variations observed in 2022 (Wang et al., 2023), anomalous reductions in mid-latitude chlorine (Cl) reservoir species hydrochloric acid (HCl) along with enhancements in reactive chlorine monoxide (ClO) (Santee et al., 2023), suggest that Cl chemistry is also likely to contribute to the record low ozone abundances in 2022.

It is well-known that the SO_2 emission from the volcanic eruptions can enhance aerosol surface areas for heterogeneous chemistry (e.g., Hofmann & Solomon, 1989; Solomon et al., 1999). As the dense volcanic aerosols of HTHH spread in the stratosphere, satellite measurements from Microwave Limb Sounder (MLS) and Optical Spectrograph and InfraRed Imager System (OSIRIS) reported large reductions in concentrations of stratospheric nitrogen oxide (NOx), via hydrolysis of dinitrogen pentoxide (N_2O_5) on aerosols (Santee et al., 2023; Zhang et al., 2023). In response, the concentration of ClO increases as less NOx is available to convert ClO into reservoir species chlorine nitrate ($ClONO_2$). Despite the large impact on NOx and ClO, N_2O_5 hydrolysis does not affect HCl to any significant degree. Previous study from Santee et al. (2023) has highlighted the role of dynamics in influencing HCl mixing ratio anomalies, particularly during the latter part of 2022. Further, tracer-tracer analysis from Wilmouth et al. (2023) shows deviations in MLS-observed HCl and N_2O relations, suggesting that the chemical losses to HCl cannot be ignored. The underlying reasons behind the chemical loss of HCl are the subject of this study.

There are a few possible pathways for the HCl chemical loss. A major mechanism contributing to the reduction of HCl involves its heterogeneous reaction on and within particles, leading to the production of highly reactive chlorine forms such as Cl_2 and HOCl (Solomon et al., 2015). Therefore, these heterogeneous processes have the capability to "activate" chlorine from the reservoirs. In the polar region, where polar stratospheric clouds (PSC) form at cold temperatures, the following heterogeneous reaction $HCl+ClONO_2 \rightarrow Cl_2+HNO_3$ (Solomon et al., 1986) occurs on PSC surface and substantially depletes HCl. This heterogenous chlorine reaction is highly temperature dependent and is only effective on the surfaces of typical stratospheric aerosols at temperatures below 195 K (Hanson et al., 1994; Shi et al., 2001; Kawa et al., 1997; Solomon et al., 2015). The atmospheric temperatures are generally too warm (>200k) for this heterogeneous reaction to take place at mid-latitudes, although Solomon et al. (2023) demonstrated this reaction could happen at warmer temperatures on organic-rich wildfire aerosols. In addition, in the presence of substantial water injections, a moist stratosphere can modify conditions favoring heterogeneous processing, as noted by Solomon et al. (1999) and Anderson et al. (2012). In the case of the HTHH eruption, increased concentrations of water vapor and sulfate in the stratosphere have the potential to elevate the threshold temperature for chlorine activation, enabling polar processing and chlorine activation occurrence in mid-latitudes. Additionally, the importance of heterogeneous bromine reactions on the stratospheric sulfate aerosol has been examined by a number of groups (e.g., Hanson et al., 1994; Hanson and Ravishankara, 1995; Abbatt, 1995; Tie and Brasseur, 1996; Slusser et al., 1997). These studies indicate that under conditions of high aerosol surface area, the reaction $HOBr+HCl \rightarrow BrCl+H_2O$ could represent a significant loss process for HCl at mid-latitudes. Later measurements reported by Waschewsky and Abbatt (1999) and Hanson (2003) support and even suggest that under warm stratospheric conditions (205-220 K), HCl loss via reaction with HOBr could become significant. The hydrolysis of bromine nitrate ($BrONO_2$) can serve as a significant source of HOBr under elevated aerosol loadings, and this reaction does not exhibit strong temperature dependence. Recent studies have also emphasized the ability of organic aerosols from wildfires to activate chlorine in the mid-latitude lower stratosphere (Santee et al., 2022; Bernath et al., 2022, Solomon et al., 2022, 2023). Thus, understanding this chemistry is also important for discriminating between volcanic and wildfire or other organic-aerosol chemistry at mid-latitudes.

Further, the conversion of HCl to reactive chlorine via the gas-phase reaction $HCl+OH \rightarrow Cl+H_2O$ can also be accelerated due to the elevated OH level in the aftermath of the HTHH eruption. The massive injection of water vapor leads to a direct and rapid increase in stratospheric OH abundances (Zhu et al., 2022). In addition, photolysis of the gas-phase HNO_3, HOCl and HOBr produced from the hydrolysis of N_2O_5, $ClONO_2$, and $BrONO_2$ is a source of reactive hydrogen, HOx ($OH + HO_2$). The reduction in NOx concentration also contributes to an increase in HOx by impeding the rate of the reaction between NO_2 and OH.

This study aims to discern whether chlorine activation primarily occurs through gas-phase or heterogeneous chemistry in the wake of HTHH, and the processes that are responsible for the chemical loss of HCl. This work will not quantify the ozone loss; rather, it will be exclusively focused on the chlorine chemistry. The ozone loss and ozone chemistry has been discussed in Zhang et al., (2023).

2. Data and Method

2.1 Satellite data

The study utilizes datasets from the Atmospheric Chemistry Experiment-Fourier Transform Spectrometer (ACE) and MLS. Level 2 satellite data from ACE version 5.2 are employed for H_2O, N_2O and HCl (Boone et al., 2005 and Boone, 2020). Additionally, daily level 3 satellite data from MLS version 5.0 are used for N_2O and HCl (Livesey et al., 2020). Both datasets span from 2007 to 2022 to match with the model simulation period. We exclude 2020-2021 because of the extreme Australian new year's wildfire in late 2019/early 2020 (Santee et al., 2022; Solomon et al., 2022, 2023; Strahan et al., 2022; Bernath et al., 2022). Anomalies for N_2O and HCl in 2022 (Figure 1) are calculated as deviations from the mean of the 2007-2019 climatological background. Livesey et al. (2021) pointed out the long-term trend of MLS N_2O is suffering from a ~3-4% per decade drift in the lower stratosphere. Here, we detrend MLS daily data to allow an interannual comparison.

2.2 Community Earth System Model Version 2 (CESM2)/Whole Atmosphere Community Climate Model (WACCM)

The numerical experiments in this study were conducted using CESM2/WACCM6, a state-of-the-art chemistry-climate model that spans from the Earth's surface to approximately 140 km. The model incorporates a comprehensive representation of troposphere-stratosphere-mesosphere-lower-thermosphere (TSMLT) chemistry, with detailed descriptions available in Gettelman et al. (2019). WACCM6 features a prognostic stratospheric aerosol module (Mills et al., 2016) and has been extensively employed to investigate the impact of volcanic aerosols on heterogeneous processes and their impact on ozone loss (e.g., Mills et al., 2017; Stone et al., 2017; Zambri et al., 2019). The reaction probabilities for key stratospheric heterogeneous processes on sulfate aerosol used in WACCM are listed in Table S1.

For this study, the simulations are characterized by a horizontal resolution of 0.9° latitude × 1.25° longitude, utilizing the finite volume dynamical core (Lin & Rood, 1996). The model includes 110 vertical levels, with a vertical resolution of approximately 500m in the upper troposphere and lower stratosphere. WACCM6 is operated in a specified dynamics configuration, where temperatures and horizontal winds (U, V) are relaxed, or nudged, to the Modern-Era Retrospective analysis for Research and Applications Version 2 (MERRA-2) reanalysis (Gelaro et al., 2017) using a relaxation timescale of 12 hours. The nudging method employed in this study follows the approach outlined by Davis et al. (2022). This configuration spans from 2007 until the end of 2022, initialized with conditions from a long historical simulation (Gettelman et al., 2019). The model setup incorporates major stratospheric volcanic injections from 2007 to 2021. Beginning in January 2022, two distinct cases are conducted: the volcano case with external forcing (SO_2 and H_2O injection) from the HTHH eruption, and the control case with no external forcing (no SO_2 nor H_2O injection) from the HTHH eruption. The disparity between these two nudged simulations provides insights into the chemistry-related changes post the HTHH eruption. This study assumes the emissions are 150 Tg H_2O and 0.6 Tg SO_2 on January 15, 2022, from approximately 20 to 35 km altitude. The injection profiles of H_2O and SO_2 are similar to Zhu et al. (2022), however, with an adjustment of SO_2 injection. The SO_2 injection estimate ranges from 0.4 Tg to 1 Tg (e.g., Millan et al., 2022; Li et al., 2023; Sellitto et al., 2023) from different sources and approaches. Here an SO_2 injection of 0.6 Tg is utilized, leading to aerosol extinction that exhibits strong agreement with the Ozone Mapping and Profiler Suite Limb Profiler (OMPS-LP) observation, especially during the 2022 Austral winter (Figure S1).

2.3 Tracer-tracer method

Exploring the correlation among chemical species, commonly known as "tracer–tracer" analysis, serves as a robust approach to dissect the interactions between dynamical and chemical processes (e.g., Proffitt et al., 1990; Griffin et al., 2019). In this study, we construct a “no-chemistry” baseline from the linear fit between N_2O and HCl over January to March data, since no or little heterogeneous chemistry normally occurs in these three months given warm conditions. The foundation of this analysis lies in the expectation that dynamical transport should impact both N_2O and HCl in a similar manner. The deviations of HCl from this “no-chemistry” baseline are defined as ΔHCl, indicating the changes in HCl that are due to chemical processes. A detailed discussion on this method can be found in Wang et al., (2023).

In this analysis, N_2O serves as an inactive tracer for calculating ΔHCl, given its availability in both ACE and MLS observations. The distinct long-term trends of N_2O and HCl resulting from anthropogenic emissions could introduce a bias in the tracer-tracer correlation. Furthermore, the drifting issue associated with MLS N_2O adds complexity to the long-term trends. To address this, ΔHCl for each year is computed based on the "no-chemistry" baseline established in that specific year. This approach prevents long-term trends in N_2O and HCl from affecting the calculations.

3. Results and Discussions

3.1 Chemical signal of HCl loss at mid-latitudes (30-55°S)

The 2022 anomalies are computed as deviations from the climatological mean, shown in Figure 1. We linearly detrend both satellite observations and model simulations using data from 2007 to 2019 to accommodate the long-term trends in N_2O and HCl as well as additional instrumental drift in MLS N_2O. The climatology encompasses various phases of the Quasi-Biennial Oscillation (QBO). Therefore, the derived stratospheric anomalies in HCl and N_2O reflect both the influence of the 2022 QBO phase and the forced changes after the HTHH eruption, including both dynamical and chemical impacts. We use N_2O, a long-lived transport tracer, to clarify the influence of dynamics in shaping the distribution of trace gasses. Notably, in much of the lower stratosphere, the vertical and meridional gradients of N_2O exhibit an opposite pattern to HCl. As a result, N_2O is generally anticorrelated with HCl in the lower stratosphere. The hatched regions on the plot denote areas where the 2022 anomalies fall outside the range of all variability during the period 2007-2019. Specifically, for N_2O and HCl, the hatches indicate that the 2022 value represents the maximum and minimum, respectively, compared to the climatological data. The WACCM N_2O anomaly is consistent with observations, suggesting that the dynamical transport on tracer distribution is represented well in WACCM.

The WACCM HCl anomaly in 2022 closely aligns with ACE and MLS relative to the climatology. These anomalies arise from a combination of internal variability and the forced dynamical and chemical changes triggered by the HTHH eruption. The onset of the negative anomaly in HCl is evident from May, corresponding to the arrival of substantial aerosols from the HTHH eruption in this region (Santee et al., 2023). During the months of June, July, and August (JJA), ACE, MLS, and WACCM consistently depict the lowest HCl levels compared to all years included in the climatology (indicated by hatching in Figure 1), consistent with the large negative HCl anomaly in winter reported in Wilmouth et al., (2023). In the latter part of the year, specifically between 17 to 27 km, both model and observations exhibit a substantial negative anomaly in HCl. Despite the

potential for chemical processing in this region, the signal of such processing is largely overshadowed by significant countervailing positive anomalies in N_2O, indicating the predominant influence of transport effects. However, in the key altitude range of approximately 19 to 23 km during JJA that we focus on here, the large HCl anomaly is not accompanied by a similarly large N_2O anomaly. This discrepancy suggests that dynamics alone cannot account for the low HCl levels in that region, and chemical processing is highly likely taking place. The subsequent analysis will focus on this specific region during the SH winter months.

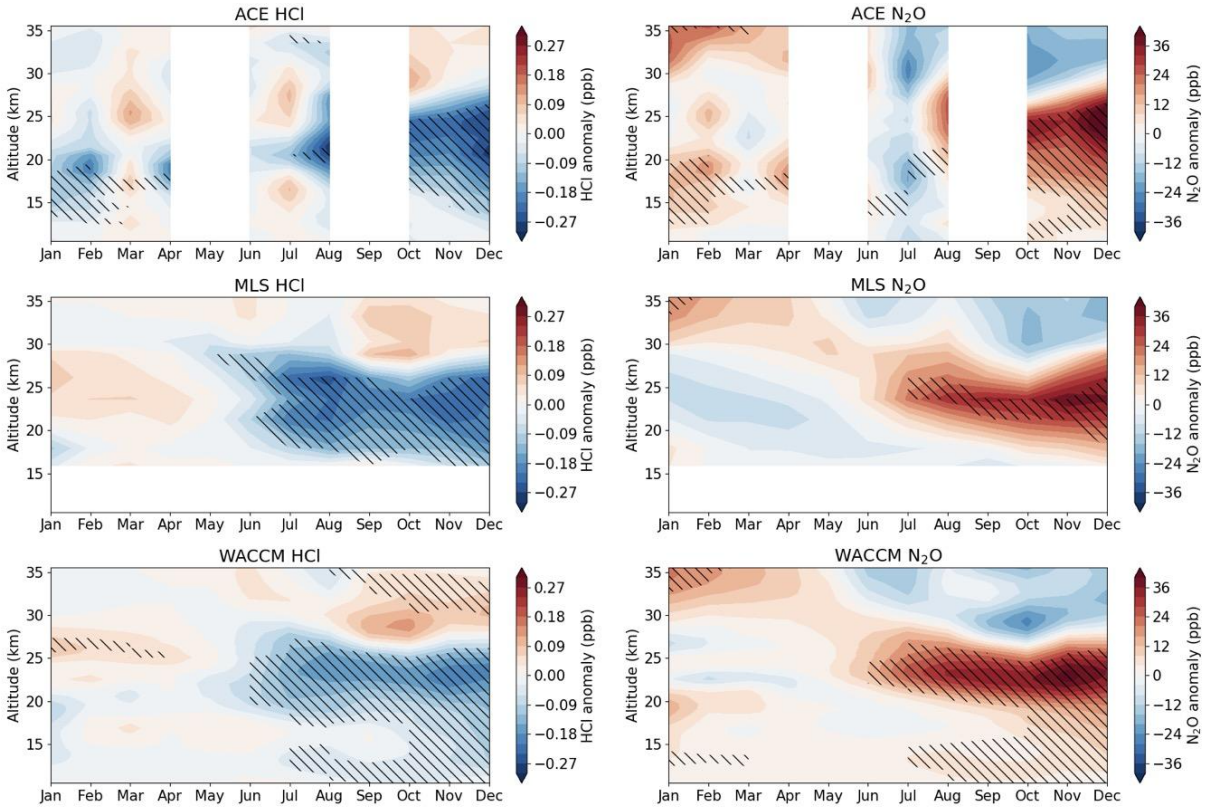

Figure 1. Calculated 2022 HCl anomaly in ppbv (left panels) and N_2O anomaly in ppbv (right panels) relative to climatology (2007 to 2019) from ACE, MLS, and WACCM in the SH mid-latitudes (30-55°S). Hatched regions indicate where the 2022 anomalies are outside the range of all variability during 2007-2019.

3.2 Significant stratospheric chlorine activation

The top panel in Figure 2 depicts the tracer-tracer relationship of ACE N_2O and HCl in June, July, August and October at 20.5 km over 30 to 55°S, color-coded by water vapor concentration. ACE doesn't have observations in May and September 2022 over this latitude range. The thick black lines in the top panel of Figure 2 represent the "no-chemistry" baseline in 2022, and the shaded area encompasses a conservative full range of baseline variability, bounded by the maximum and minimum baselines between 2007 and 2019. Deviations from correlation observed in HCl suggest the presence of chemical processes, as described in Wang et al. (2023). The intensity of chemical processes becomes more pronounced with greater deviations of HCl from the baseline. Tracer-tracer plots further confirm the strong chemical processing that occurs in June and intensifies in

July and August in 2022 compared to 2007 to 2019 (triangles in Figure 2). It is notable that deviations in HCl from their respective "no-chemistry" baseline occur in June to August from 2007 to 2019 (round points in Figure 2), as chlorine activation happens every year in these months with a seasonal cycle. In October, Cl activation slows down as the polar spring advances with temperature rise, thus the HCl departure from the baseline reduces.

The bottom panel of Figure 2 displays the derived ΔHCl resulting from chemical processes from MLS, ACE, and WACCM in 2022. ACE and MLS ΔHCl is calculated by the deviations from the baseline, with the seasonal cycle removed. The shaded regions in blue and red represent the range of ±1 standard deviation (std) for MLS and ACE, respectively, for each month from 2007 to 2019. The patterns of derived ΔHCl from observations closely resemble those calculated by WACCM from the two nudged simulations (volcano minus control). Notably, the largest chemical induced HCl reduction occurs in the SH winter. Figure 2 further indicates that tracer-tracer analysis can effectively be employed to derive ΔHCl due to chemical processes using MLS and ACE data, and the results exhibit comparability with those from the chemistry climate model. The differences between WACCM, ACE and MLS are within the uncertainty range (±1 std).

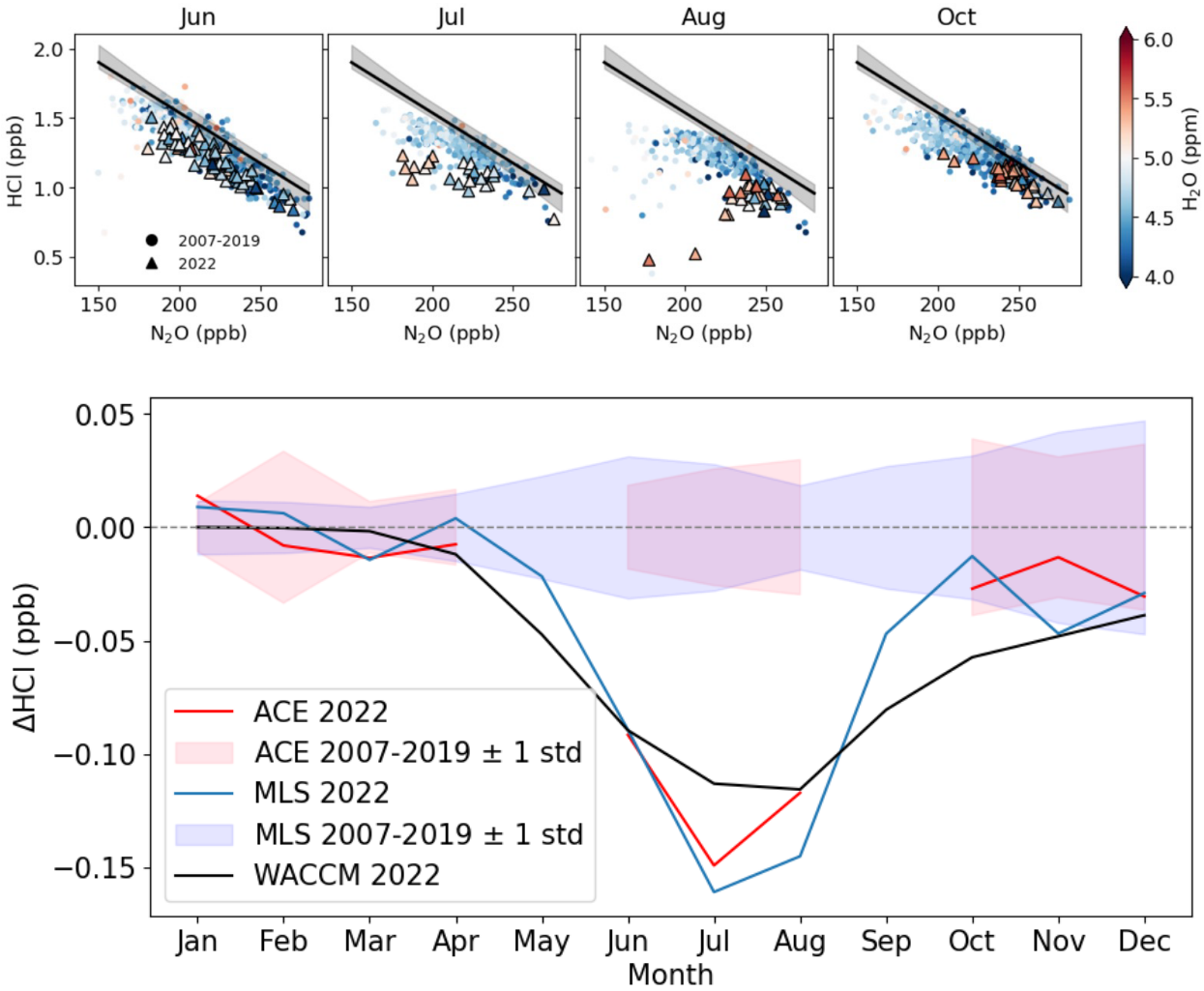

Figure 2. Top panel: Tracer–tracer correlation between ACE-measured N_2O (x-axis) and HCl (y-axis), color-coded by water vapor concentration. Each dot represents a single measurement at 20.5 km over 30 to 55°S. The thick black lines represent the no-chemistry baseline, from the linear fit over January to March 2022 data points. The shaded regions indicate a conservative full range of baseline variability bounded by the maximum and minimum baselines constructed by data in individual years from 2007 to 2019. Bottom panel: Calculated ΔHCl from ACE, MLS and WACCM in 2022 averaging all points over 30 to 55°S. ACE and MLS ΔHCl is calculated from departures from the baseline in the top panel but with the seasonal cycle removed, representing the change in HCl due to anomalous chemical processes in 2022. The blue and red shaded regions indicate ±1 standard deviation range for MLS and ACE in each month from 2007 to 2019. WACCM ΔHCl is calculated from the difference in HCl between the volcano and the control run.

3.3 Role of gas and heterogenous phase chemistry in chlorine activation

To understand the chemical processes that give rise to the ΔHCl in Figure 2 following the HTHH eruption, a thorough model examination is conducted. Figure 3 illustrates the changes in gas-phase

and heterogeneous-phase chemistry, along with the cumulative changes of all chemistry. The ΔHCl is calculated from the volcano case compared to the control case. Gas-phase chemistry (Figure 3a) results in an increase in HCl below 23 km over the 30 to 55°S, accompanied by a decrease from 23 to 30 km. Heterogeneous chemistry (Figure 3b) induces HCl depletion from 15 to 25 km. Considering both gas and heterogeneous chemistry (Figure 3c), the ΔHCl exhibits a net reduction above 19 km from April to December, with the maximum reduction occurring in the winter, consistent with Figure 2. There is an HCl increase below 18 km (Figure 3c), attributable to enhanced gas-phase reactions, particularly Cl+CH_4 and ClO+OH (discussed below).

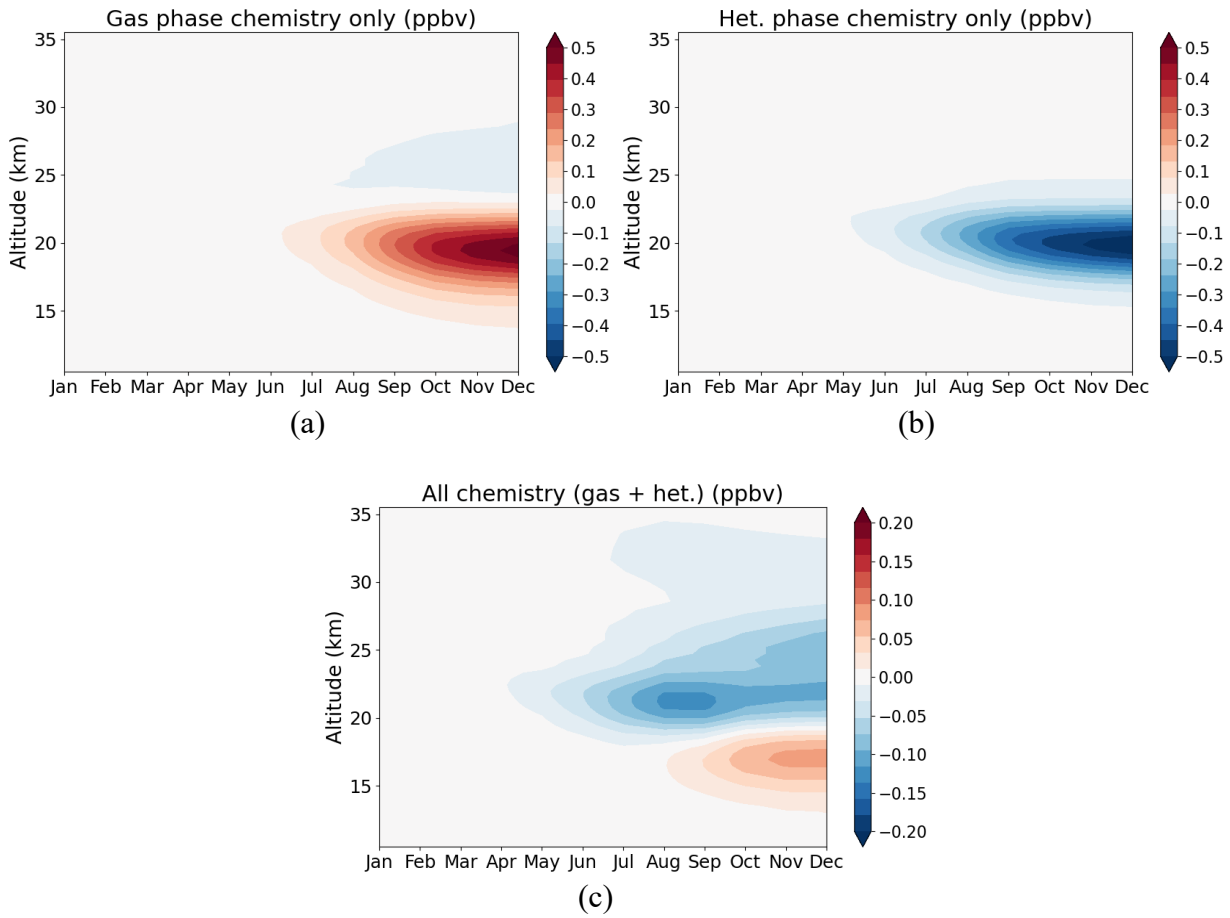

Figure 3. WACCM calculated ΔHCl (ppbv) from the volcano minus the control case for (a) gas-phase chemistry only, (b) heterogeneous chemistry only and (c) the sum of all gas and heterogeneous chemistry over 30 to 55°S. Note that panels c has different color bar ranges from panels a and b.

Perturbations in individual reactions are investigated following the HTHH eruption, with a particular focus during JJA. The ones with important contributions to the ΔHCl are plotted in Figure 4 with different colors. The rest of the reactions only affect less than 1% of ΔHCl, thus are not shown here. A full list of HCl reactions examined can be found in Table S2. The "all gas" black line in Figure 4a adds up all the gas reactions, not just the gas terms plotted in the figures, and same for the "all het" black line in Figure 4b. In the realm of gas-phase chemistry (Figure 4a), the reaction between HCl and elevated OH acts as a significant sink for HCl from the simulated

perturbation due to HTHH. However, this loss is entirely compensated for by the heightened gas-phase production, particularly $Cl+CH_4$ and ClO+OH. Among heterogeneous reactions (Figure 4b), the primary sink for HCl is the reaction between HOBr and HCl on sulfate aerosols between 15 to 25 km, with $ClONO_2$+HCl contributing as well, albeit with a much smaller magnitude. This is mainly attributed to volcanic aerosols providing additional surface area density (SAD) for heterogeneous chemistry at these altitudes (Figure 4d). Here we conclude that, during the SH wintertime, the HCl chemical reduction from 15 to 24 km in the mid-latitudes is attributed to heterogeneous chemistry rather than gas-phase chemistry (Figure 4c). Our results for this season differ from the findings reported by Wilmouth et al. (2023), where they suggest that gas-phase chemistry is the primary cause of the chemical loss of HCl. They state that this is because of the enhanced HCl loss with elevated OH, as well as the slower HCl production from $Cl+CH_4$ reaction. Our findings support the former but not the latter, resulting in a different net effect for gas-phase reactions alone.

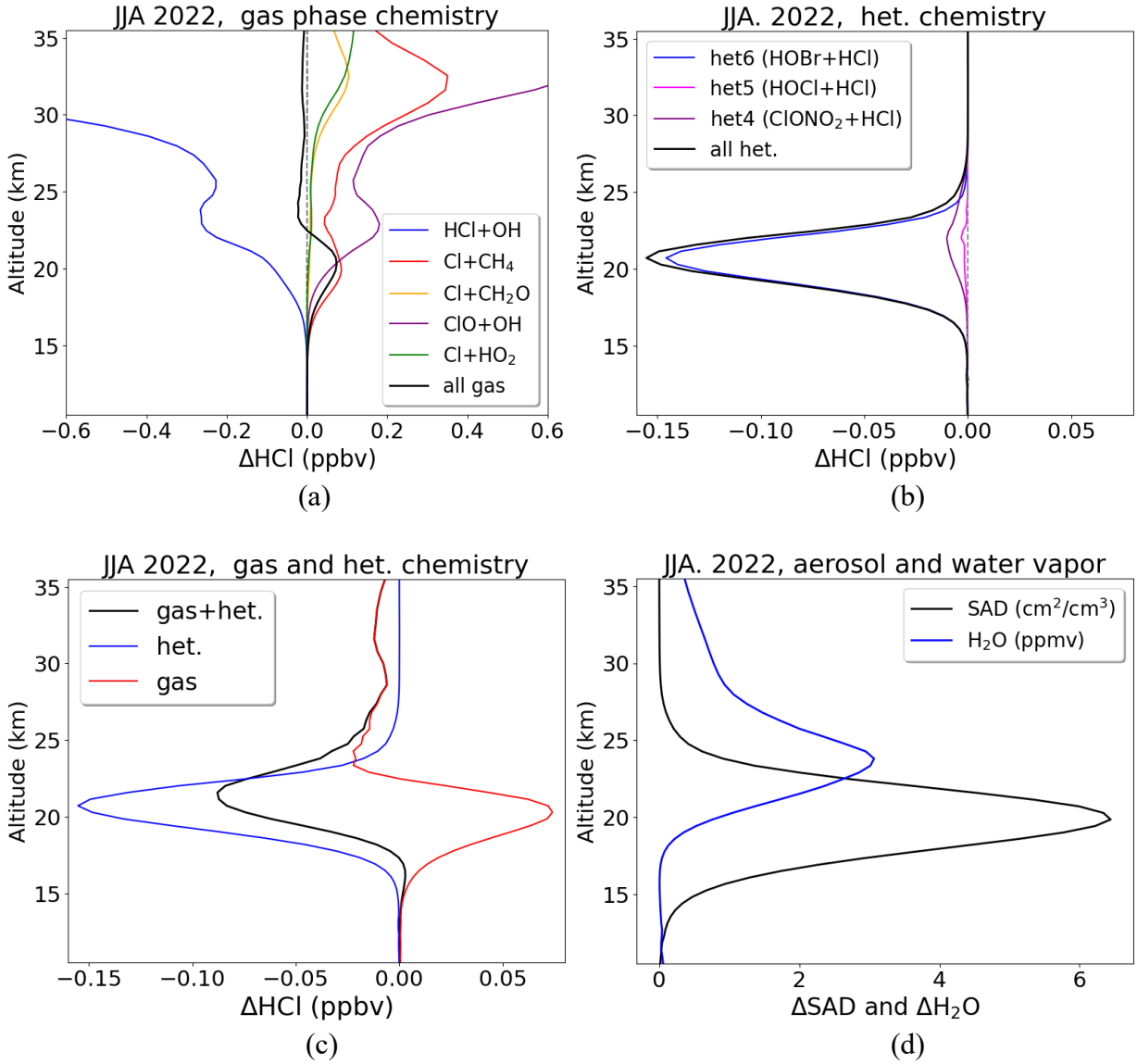

Figure 4. ΔHCl (in ppbv) contribution from individual reactions for (a) gas chemistry, (b) heterogeneous chemistry and (c) the sum of all chemistry averaged over JJA in 2022 over 30 to 55°S. ΔHCl is calculated from the volcano minus control case. (d) the modeled aerosol surface area density in um^2/cm^3 and water in ppmv.

The injection of volcanic water and aerosols from the HTHH eruption perturbs atmospheric conditions (e.g., surface area density, aerosol radiance and H_2SO_4 content), which further impact the reactive probability of heterogeneous reactions. Comparative analysis between the volcano case and the control case reveals enhanced reactive probabilities for all examined heterogeneous reactions in the volcano scenario (Figure S2). Laboratory studies (Hanson and Ravishankara, 1995; Hanson et al., 1996, 2003) have demonstrated the highly efficient hydrolysis of $BrONO_2$ in sulfuric acid solutions. Reaction probabilities of approximately 0.8 were documented for the uptake of $BrONO_2$ onto sulfuric acid solutions with H_2SO_4 content ranging from 40 to 70 weight percentage (wt%) (Figure S2). The enhanced water concentration at mid-latitudes doesn't substantially decrease the sulfuric acid content during the SH winter, unlike immediately after the eruption when the massive influx of water reduces the weight percent of H_2SO_4 from 70% to 35% (Zhu et al., 2023). Compared to other heterogeneous processes, hydrolysis of $BrONO_2$ is relatively temperature-insensitive and can take place rapidly at various stratospheric conditions, making their influence important and widespread. The product resulting from the hydrolysis of $BrONO_2$, HOBr, undergoes another heterogeneous process with HCl, providing an additional pathway to chlorine activation. Under temperatures in the mid-latitudes (>200K), the enhancement in the rate of HOBr+HCl reactions after the HTHH eruption plays a dominant role in HCl depletion among all the heterogeneous processes.

4. Summary and discussion

In summary, we have examined the mid-latitudes HCl reduction in the SH winter following the eruption of HTHH using satellite data and global chemistry-climate model. Our analysis indicates a significant role for heterogeneous chemical processing in the observed HCl reduction. The results confirm that the tracer-tracer method provides a good estimate of the chemical impacts distinct from dynamics. And the derived chemical HCl change is consistent among ACE, MLS and WACCM. Further delving into WACCM's detailed chemistry, we examine individual chlorine gas-phase and heterogeneous reactions. We find that despite a substantial increase in the reaction of HCl with elevated OH in the SH winter, this loss is entirely compensated for by heightened gas-phase production from $Cl+CH_4$ and ClO+OH. Heterogeneous chemistry emerges as the primary driver for the chemical loss of HCl, with the reaction between HOBr and HCl on sulfate aerosols identified as the most crucial process. Our study provides useful information for understanding volcanic impacts on stratospheric chemistry, particularly their detailed breakdown among gas-phase and heterogeneous reactions at mid-latitudes.

Acknowledgments

Jun Zhang is supported by the NSF via NCAR's Advanced Study Program Postdoctoral Fellowship. Douglas Kinnison is partially supported by NASA grant no. 80NSSC19K0952. Peidong Wang, Susan Solomon and Jian Guan gratefully acknowledge support by NSF-AGS [2316980]. NCAR's Community Earth System Model project is supported primarily by the National Science Foundation. This material is based upon work supported by the NSF National Center for Atmospheric Research, which is a major facility sponsored by the U.S. National Science Foundation under Cooperative Agreement No. 1852977. Computing and data storage resources, including the Cheyenne supercomputer (doi:10.5065/D6RX99HX), were provided by the Computational and Information Systems Laboratory (CISL) at NCAR. This project received

funding from NOAA's Earth Radiation Budget (ERB) Initiative (CPO #03-01-07-001). Yunqian Zhu is supported in part by NOAA cooperative agreements NA17OAR4320101 and NA22OAR4320151.

Open Research

CESM2/WACCM6 (described in Gettelman et al., 2019) is an open-source community model, which was developed with support primarily from the National Science Foundation. Figures in this study are plotted using an open-source software Python. The atmospheric modeling dataset used in the analysis is published (Zhang et al., 2024).

References

Abbatt, J. P. (1995). Interactions of HBr, HCl, and HOBr with supercooled sulfuric acid solutions of stratospheric composition. *Journal of Geophysical Research: Atmospheres*, 100(D7), 14009-14017.

Anderson, J. G., Wilmouth, D. M., Smith, J. B., & Sayres, D. S. (2012). UV dosage levels in summer: Increased risk of ozone loss from convectively injected water vapor. *Science*, 337(6096), 835-839.

Bernath, P., Boone, C., & Crouse, J. (2022). Wildfire smoke destroys stratospheric ozone. *Science*, 375(6586), 1292-1295.

Carn, S. A., Krotkov, N. A., Fisher, B. L., & Li, C. (2022). Out of the blue: Volcanic SO2 emissions during the 2021–2022 eruptions of Hunga Tonga—Hunga Ha'apai (Tonga). *Frontiers in Earth Science*, 10, 976962. https://doi.org/10.3389/feart.2022.976962

Davis, N. A., Callaghan, P., Simpson, I. R., & Tilmes, S. (2022). Specified dynamics scheme impacts on wave-mean flow dynamics, convection, and tracer transport in CESM2 (WACCM6). *Atmospheric Chemistry and Physics*, 22(1), 197-214. https://doi.org/10.5194/acp-22-197-2022

Gelaro, R., McCarty, W., Suárez, M. J., Todling, R., Molod, A., Takacs, L., ... & Zhao, B. (2017). The modern-era retrospective analysis for research and applications, version 2 (MERRA-2). *Journal of climate*, 30(14), 5419-5454. https://doi.org/10.1175/JCLI-D-16-0758.1

Gettelman, A., Mills, M. J., Kinnison, D. E., Garcia, R. R., Smith, A. K., Marsh, D. R., ... & Randel, W. J. (2019). The whole atmosphere community climate model version 6 (WACCM6). *Journal of Geophysical Research: Atmospheres*, 124(23), 12380-12403. https://doi.org/10.1029/2019JD030943

Griffin, D., Walker, K. A., Wohltmann, I., Dhomse, S. S., Rex, M., Chipperfield, M. P., ... & Tarasick, D. (2019). Stratospheric ozone loss in the Arctic winters between 2005 and 2013 derived with ACE-FTS measurements. *Atmospheric Chemistry and Physics*, 19(1), 577-601.

Mills, M. J., Kinnison, D. E., Garcia, R. R., Smith, A. K., Marsh, D. R., ... & Randel, W. J. (2019). The whole atmosphere community climate model version 6 (WACCM6). *Journal of Geophysical Research: Atmospheres*, 124(23), 12380-12403. https://doi.org/10.1029/2019JD030943

Hanson, D. R., Ravishankara, A. R., & Solomon, S. (1994). Heterogeneous reactions in sulfuric acid aerosols: A framework for model calculations. *Journal of Geophysical Research: Atmospheres*, 99(D2), 3615-3629.

Hanson, D. R., & Ravishankara, A. R. (1995). Heterogeneous chemistry of bromine species in sulfuric acid under stratospheric conditions. *Geophysical research letters*, 22(4), 385-388.

Hanson, D. R., Ravishankara, A. R., & Lovejoy, E. R. (1996). Reaction of BrONO2 with H2O on submicron sulfuric acid aerosol and the implications for the lower stratosphere. *Journal of Geophysical Research: Atmospheres*, 101(D4), 9063-9069.

Hanson, D. R. (2003). Reactivity of BrONO2 and HOBr on sulfuric acid solutions at low temperatures. *Journal of Geophysical Research: Atmospheres*, 108(D8).

Hofmann, D. J., & Solomon, S. (1989). Ozone destruction through heterogeneous chemistry following the eruption of El Chichon. *Journal of Geophysical Research: Atmospheres*, 94(D4), 5029-5041. https://doi.org/10.1029/JD094iD04p05029

Kawa, S. R., Newman, P. A., Lait, L. R., Schoeberl, M. R., Stimpfle, R. M., Kohn, D. W., ... & Loewenstein, M. (1997). Activation of chlorine in sulfate aerosol as inferred from aircraft observations. *Journal of Geophysical Research: Atmospheres*, 102(D3), 3921-3933.

Li, Z., Bi, J., Hu, Z., Ma, J., & Li, B. (2023). Regional transportation and influence of atmospheric aerosols triggered by Tonga volcanic eruption. *Environmental Pollution*, 325, 121429.

Lin, S. J., & Rood, R. B. (1996). Multidimensional flux-form semi-Lagrangian transport schemes. *Monthly Weather Review*, 124(9), 2046-2070. https://doi.org/10.1175/1520-0493(1996)124<2046:MFFSLT>2.0.CO;2

Livesey, N J, W G Read, P A Wagner, L Froidevaux, M L Santee, and M J Schwartz. 2020. "Version 5.0 x Level 2 and 3 Data Quality and Description Document (Tech. Rep. No. JPL D-105336 Rev. A)." *Jet Propulsion Laboratory*.

Livesey, N. J., Read, W. G., Froidevaux, L., Lambert, A., Santee, M. L., Schwartz, M. J., ... & Nedoluha, G. E. (2021). Investigation and amelioration of long-term instrumental drifts in water vapor and nitrous oxide measurements from the Aura Microwave Limb Sounder (MLS) and their implications for studies of variability and trends. *Atmospheric Chemistry and Physics*, 21(20), 15409-15430.

Millan, L., Santee, M. L., Lambert, A., Livesey, N. J., Werner, F., Schwartz, M. J., ... & Froidevaux, L. (2022). The Hunga Tonga-Hunga Ha'apai hydration of the stratosphere. *Geophysical Research Letters*, 49(13), e2022GL099381. https://doi.org/10.1029/2022GL099381

Mills, M. J., Schmidt, A., Easter, R., Solomon, S., Kinnison, D. E., Ghan, S. J., ... & Gettelman, A. (2016). Global volcanic aerosol properties derived from emissions, 1990–2014, using CESM1 (WACCM). *Journal of Geophysical Research: Atmospheres*, 121(5), 2332-2348. https://doi.org/10.1002/2015JD024290

Mills, M. J., Richter, J. H., Tilmes, S., Kravitz, B., MacMartin, D. G., Glanville, A. A., ... & Kinnison, D. E. (2017). Radiative and chemical response to interactive stratospheric sulfate aerosols in fully coupled CESM1 (WACCM). *Journal of Geophysical Research: Atmospheres*, 122(23), 13-061. https://doi.org/10.1002/2017JD027006

Proffitt, M. H., Margitan, J. J., Kelly, K. K., Loewenstein, M., Podolske, J. R., & Chan, K. R. (1990). Ozone loss in the Arctic polar vortex inferred from high-altitude aircraft measurements. *Nature*, 347(6288), 31-36.

Randel, W. J., Johnston, B. R., Braun, J. J., Sokolovskiy, S., Vömel, H., Podglajen, A., & Legras, B. (2023). Stratospheric Water Vapor from the Hunga Tonga–Hunga Ha'apai Volcanic Eruption Deduced from COSMIC-2 Radio Occultation. *Remote Sensing*, 15(8), 2167. https://doi.org/10.3390/rs15082167

Santee, M. L., Lambert, A., Froidevaux, L., Manney, G. L., Schwartz, M. J., Millán, L. F., et al. (2023). Strong evidence of heterogeneous processing on stratospheric sulfate aerosol in the extrapolar Southern Hemisphere following the 2022 Hunga Tonga-Hunga Ha'apai eruption. *Journal of Geophysical Research: Atmospheres*, 128, e2023JD039169. https://doi.org/10.1029/2023JD039169

Sellitto, P., Siddans, R., Belhadji, R., Carboni, E., Legras, B., Podglajen, A., ... & Kerridge, B. (2023). Observing the SO2 and Sulphate Aerosol Plumes from the 2022 Hunga Tonga-Hunga Ha'apai Eruption with IASI. *Authorea Preprints*.

Shi, Q., Jayne, J. T., Kolb, C. E., Worsnop, D. R., & Davidovits, P. (2001). Kinetic model for reaction of ClONO2 with H2O and HCl and HOCl with HCl in sulfuric acid solutions. *Journal of Geophysical Research: Atmospheres,* 106(D20), 24259-24274.

Slusser, J. R., Fish, D. J., Strong, E. K., Jones, R. L., Roscoe, H. K., & Sarkissian, A. (1997). Five years of NO2 vertical column measurements at Faraday (65 S): Evidence for the hydrolysis of BrONO2 on Pinatubo aerosols. *Journal of Geophysical Research: Atmospheres*, 102(D11), 12987-12993.

Solomon, S., Garcia, R. R., Rowland, F. S., & Wuebbles, D. J. (1986). On the depletion of Antarctic ozone. *Nature*, 321(6072), 755-758.

Solomon, S. (1999). Stratospheric ozone depletion: A review of concepts and history. *Reviews of geophysics*, 37(3), 275-316. https://doi.org/10.1029/1999RG900008

Solomon, S., Kinnison, D., Bandoro, J., & Garcia, R. (2015). Simulation of polar ozone depletion: An update. *Journal of Geophysical Research: Atmospheres*, 120(15), 7958-7974. https://doi.org/10.1002/2015JD023365

Solomon, S., Stone, K., Yu, P., Murphy, D. M., Kinnison, D., Ravishankara, A. R., & Wang, P. (2023). Chlorine activation and enhanced ozone depletion induced by wildfire aerosol. Nature, 615(7951), 259-264.

Stone, K. A., Solomon, S., Kinnison, D. E., Pitts, M. C., Poole, L. R., Mills, M. J., ... & Hagiya, S. (2017). Observing the impact of Calbuco volcanic aerosols on South Polar ozone depletion in 2015. *Journal of Geophysical Research: Atmospheres*, 122(21), 11-862. https://doi.org/10.1002/2017JD026987

Taha, G., Loughman, R., Colarco, P. R., Zhu, T., Thomason, L. W., & Jaross, G. (2022). Tracking the 2022 Hunga Tonga-Hunga Ha'apai aerosol cloud in the upper and middle stratosphere using space-based observations. *Geophysical Research Letters*, 49(19), e2022GL100091. https://doi.org/10.1029/2022GL100091

Tie, X., & Brasseur, G. (1996). The importance of heterogeneous bromine chemistry in the lower stratosphere. *Geophysical research letters*, 23(18), 2505-2508.

Wang, P., Solomon, S., & Stone, K. (2023). Stratospheric chlorine processing after the 2020 Australian wildfires derived from satellite data. *Proceedings of the National Academy of Sciences*, 120(11), e2213910120.

Wang, X., Randel, W., Zhu, Y., Tilmes, S., Starr, J., Yu, W., ... & Li, J. (2023). Stratospheric Climate Anomalies and Ozone Loss Caused by the Hunga Tonga-Hunga Ha'apai Volcanic Eruption. *Journal of Geophysical Research: Atmospheres*, 128(22), e2023JD039480. https://doi.org/10.1029/2023JD039480

Waschewsky, G. C., & Abbatt, J. P. (1999). HOBr in sulfuric acid solutions: Solubility and reaction with HCl as a function of temperature and concentration. *The Journal of Physical Chemistry A*, 103(27), 5312-5320.

Wilmouth, D. M., Østerstrøm, F. F., Smith, J. B., Anderson, J. G., & Salawitch, R. J. (2023). Impact of the Hunga Tonga volcanic eruption on stratospheric composition. *Proceedings of the National Academy of Sciences*, 120(46), e2301994120.

Zambri, B., Solomon, S., Kinnison, D. E., Mills, M. J., Schmidt, A., Neely III, R. R., ... & Roth, C. Z. (2019). Modeled and observed volcanic aerosol control on stratospheric NOy and Cly. *Journal of Geophysical Research: Atmospheres*, 124(17-18), 10283-10303. https://doi.org/10.1029/2019JD031111

Zhang, J., Kinnison, D. E., Zhu, Y., Wang, X., Tilmes, S., Dubé, K. R., & Randel, W. J. (2023). Chemistry contribution to stratospheric ozone depletion after the unprecedented water rich Hunga Tonga eruption. *Authorea Preprints*.

Zhang, J., Kinnison, D., Zhu, Y., Wang, X., Tilmes, S., Dube, K., Randel, W., (Version 1.0.) [Dataset] (2023). UCAR/NCAR - GDEX. https://doi.org/10.5065/nsar-fh76

Zhang, J., Wang, P., Kinnison, D., Solomon, S., Guan, J., Zhu, Y., (Version 1.0.) [Dataset] (2024). UCAR/NCAR - GDEX. https://doi.org/10.5065/j6yg-a009

Zhu, Y., Bardeen, C. G., Tilmes, S., Mills, M. J., Wang, X., Harvey, V. L., ... & Toon, O. B. (2022). Perturbations in stratospheric aerosol evolution due to the water-rich plume of the 2022 Hunga-Tonga eruption. *Communications Earth & Environment*, 3(1), 248. https://doi.org/10.1038/s43247-022-00580-w

Zhu, Y., Portmann, R. W., Kinnison, D., Toon, O. B., Millán, L., Zhang, J., ... & Rosenlof, K. H. (2023). Stratospheric ozone depletion inside the volcanic plume shortly after the 2022 Hunga Tonga eruption. *Atmospheric Chemistry and Physics*, 23(20), 13355-13367.

Stratospheric chlorine processing after the unprecedented Hunga Tonga eruption

Authors: Jun Zhang[1*], Peidong Wang[2], Douglas Kinnison[1], Susan Solomon[2], Jian Guan[2], Yunqian Zhu[3,4]

Affiliations:

[1]Atmospheric Chemistry Observations & Modeling Laboratory, NSF National Center for Atmospheric Research, Boulder, CO, USA

[2] Department of Earth, Atmospheric, and Planetary Sciences, Massachusetts Institute of Technology, Cambridge, MA, USA, 02139

[3] Cooperative Institute for Research in Environmental Sciences, University of Colorado Boulder, Boulder, CO, USA, 80309

[4]Chemical Sciences Laboratory, National Oceanic and Atmospheric Administration, Boulder, CO, USA, 80305

[*]Corresponding author: Jun Zhang (jzhan166@ucar.edu)

Key Points:

- A significant reduction in stratospheric HCl was observed in the Southern Hemisphere mid-latitudes during the latter half of 2022.
- Analysis using both model and satellites suggest a significant role of chemical processing in the observed HCl reduction.
- Heterogeneous chemistry is the primary driver for the chemical HCl loss, with HOBr + HCl on sulfate aerosols as the dominant process.

Abstract

Following the Hunga Tonga–Hunga Ha'apai (HTHH) eruption in January 2022, a significant reduction in stratospheric hydrochloric acid (HCl) was observed in the Southern Hemisphere mid-latitudes during the latter half of 2022, suggesting potential chlorine activation. The objective of this study is to comprehensively understand the substantial loss of HCl in the aftermath of HTHH. Satellite measurements along with a global chemistry-climate model are employed for the analysis. We find strong agreement of 2022 anomalies between the modeled and the measured data. The observed tracer-tracer relations between N_2O and HCl indicate a significant role of chemical processing in the observed HCl reduction, especially during the austral winter of 2022. Further examining the roles of chlorine gas-phase and heterogeneous chemistry, we find that heterogeneous chemistry emerges as the primary driver for the chemical loss of HCl, with the reaction between HOBr and HCl on sulfate aerosols identified as the dominant loss process.

Plain language summary

After the eruption of Hunga Tonga–Hunga Ha'apai (HTHH) in January 2022, there was a substantial decrease in stratospheric hydrochloric acid (HCl) in the Southern Hemisphere mid-latitudes in the latter part of 2022, hinting at potential chlorine activation. This study aims to comprehensively understand the significant loss of HCl following the HTHH eruption, utilizing satellite measurements and a global chemistry-climate model for analysis. The anomalies in 2022 show remarkable agreement between the modeled and measured data. Tracer-tracer relations between N_2O and HCl suggest a substantial influence of chemical processing in the observed reduction of HCl, particularly during the austral winter of 2022. Upon further investigation into the role of chlorine gas-phase and heterogeneous chemistry, heterogeneous chemistry emerges as the primary driver for the chemical loss of HCl. The reaction between HOBr and HCl on sulfate aerosols is identified as the dominant process leading to this loss.

1. Introduction

The January 2022 Hunga Tonga–Hunga Ha'apai (HTHH) eruption (20.5°S, 175.4°W) was an unprecedented underwater volcanic event in the modern era. The eruption injected about 150 Tg of water (H_2O) (Millán et al., 2022; Randel et al., 2023) along with a moderate amount of sulfur dioxide (SO_2) into the stratosphere (Carn et al. 2022; Taha et al., 2022). Satellite observations (Santee et al., 2023) and model simulations (Zhang et al., 2023; Wilmouth et al., 2023), all found significant ozone decreases in the lower stratosphere at southern hemisphere (SH) mid-latitudes in 2022 after the eruption. In particular, a record low ozone relative to the climatology (2004 to 2021) in the SH austral winter between 30 to 50 hPa was observed in the mid-latitudes (Zhang et al., 2023). While there is evidence for some dynamical contributions to the ozone variations observed in 2022 (Wang et al., 2023), anomalous reductions in mid-latitude chlorine (Cl) reservoir species hydrochloric acid (HCl) along with enhancements in reactive chlorine monoxide (ClO) (Santee et al., 2023), suggest that Cl chemistry is also likely to contribute to the record low ozone abundances in 2022.

It is well-known that the SO_2 emission from the volcanic eruptions can enhance aerosol surface areas for heterogeneous chemistry (e.g., Hofmann & Solomon, 1989; Solomon et al., 1999). As the dense volcanic aerosols of HTHH spread in the stratosphere, satellite measurements from Microwave Limb Sounder (MLS) and Optical Spectrograph and InfraRed Imager System (OSIRIS) reported large reductions in concentrations of stratospheric nitrogen oxide (NOx), via hydrolysis of dinitrogen pentoxide (N_2O_5) on aerosols (Santee et al., 2023; Zhang et al., 2023). In response, the concentration of ClO increases as less NOx is available to convert ClO into reservoir species chlorine nitrate ($ClONO_2$). Despite the large impact on NOx and ClO, N_2O_5 hydrolysis does not affect HCl to any significant degree. Previous study from Santee et al. (2023) has highlighted the role of dynamics in influencing HCl mixing ratio anomalies, particularly during the latter part of 2022. Further, tracer-tracer analysis from Wilmouth et al. (2023) shows deviations in MLS-observed HCl and N_2O relations, suggesting that the chemical losses to HCl cannot be ignored. The underlying reasons behind the chemical loss of HCl are the subject of this study.

There are a few possible pathways for the HCl chemical loss. A major mechanism contributing to the reduction of HCl involves its heterogeneous reaction on and within particles, leading to the production of highly reactive chlorine forms such as Cl_2 and HOCl (Solomon et al., 2015). Therefore, these heterogeneous processes have the capability to "activate" chlorine from the reservoirs. In the polar region, where polar stratospheric clouds (PSC) form at cold temperatures, the following heterogeneous reaction $HCl+ClONO_2 \rightarrow Cl_2+HNO_3$ (Solomon et al., 1986) occurs on PSC surface and substantially depletes HCl. This heterogenous chlorine reaction is highly temperature dependent and is only effective on the surfaces of typical stratospheric aerosols at temperatures below 195 K (Hanson et al., 1994; Shi et al., 2001; Kawa et al., 1997; Solomon et al., 2015). The atmospheric temperatures are generally too warm (>200k) for this heterogeneous reaction to take place at mid-latitudes, although Solomon et al. (2023) demonstrated this reaction could happen at warmer temperatures on organic-rich wildfire aerosols. In addition, in the presence of substantial water injections, a moist stratosphere can modify conditions favoring heterogeneous processing, as noted by Solomon et al. (1999) and Anderson et al. (2012). In the case of the HTHH eruption, increased concentrations of water vapor and sulfate in the stratosphere have the potential to elevate the threshold temperature for chlorine activation, enabling polar processing and chlorine activation occurrence in mid-latitudes. Additionally, the importance of heterogeneous bromine reactions on the stratospheric sulfate aerosol has been examined by a number of groups (e.g., Hanson et al., 1994; Hanson and Ravishankara, 1995; Abbatt, 1995; Tie and Brasseur, 1996; Slusser et al., 1997). These studies indicate that under conditions of high aerosol surface area, the reaction $HOBr+HCl \rightarrow BrCl+H_2O$ could represent a significant loss process for HCl at mid-latitudes. Later measurements reported by Waschewsky and Abbatt (1999) and Hanson (2003) support and even suggest that under warm stratospheric conditions (205-220 K), HCl loss via reaction with HOBr could become significant. The hydrolysis of bromine nitrate ($BrONO_2$) can serve as a significant source of HOBr under elevated aerosol loadings, and this reaction does not exhibit strong temperature dependence. Recent studies have also emphasized the ability of organic aerosols from wildfires to activate chlorine in the mid-latitude lower stratosphere (Santee et al., 2022; Bernath et al., 2022, Solomon et al., 2022, 2023). Thus, understanding this chemistry is also important for discriminating between volcanic and wildfire or other organic-aerosol chemistry at mid-latitudes.

Further, the conversion of HCl to reactive chlorine via the gas-phase reaction $HCl+OH \rightarrow Cl+H_2O$ can also be accelerated due to the elevated OH level in the aftermath of the HTHH eruption. The massive injection of water vapor leads to a direct and rapid increase in stratospheric OH abundances (Zhu et al., 2022). In addition, photolysis of the gas-phase HNO_3, HOCl and HOBr produced from the hydrolysis of N_2O_5, $ClONO_2$, and $BrONO_2$ is a source of reactive hydrogen, HOx ($OH + HO_2$). The reduction in NOx concentration also contributes to an increase in HOx by impeding the rate of the reaction between NO_2 and OH.

This study aims to discern whether chlorine activation primarily occurs through gas-phase or heterogeneous chemistry in the wake of HTHH, and the processes that are responsible for the chemical loss of HCl. This work will not quantify the ozone loss; rather, it will be exclusively focused on the chlorine chemistry. The ozone loss and ozone chemistry has been discussed in Zhang et al., (2023).

2. Data and Method

2.1 Satellite data

The study utilizes datasets from the Atmospheric Chemistry Experiment-Fourier Transform Spectrometer (ACE) and MLS. Level 2 satellite data from ACE version 5.2 are employed for H_2O, N_2O and HCl (Boone et al., 2005 and Boone, 2020). Additionally, daily level 3 satellite data from MLS version 5.0 are used for N_2O and HCl (Livesey et al., 2020). Both datasets span from 2007 to 2022 to match with the model simulation period. We exclude 2020-2021 because of the extreme Australian new year's wildfire in late 2019/early 2020 (Santee et al., 2022; Solomon et al., 2022, 2023; Strahan et al., 2022; Bernath et al., 2022). Anomalies for N_2O and HCl in 2022 (Figure 1) are calculated as deviations from the mean of the 2007-2019 climatological background. Livesey et al. (2021) pointed out the long-term trend of MLS N_2O is suffering from a ~3-4% per decade drift in the lower stratosphere. Here, we detrend MLS daily data to allow an interannual comparison.

2.2 Community Earth System Model Version 2 (CESM2)/Whole Atmosphere Community Climate Model (WACCM)

The numerical experiments in this study were conducted using CESM2/WACCM6, a state-of-the-art chemistry-climate model that spans from the Earth's surface to approximately 140 km. The model incorporates a comprehensive representation of troposphere-stratosphere-mesosphere-lower-thermosphere (TSMLT) chemistry, with detailed descriptions available in Gettelman et al. (2019). WACCM6 features a prognostic stratospheric aerosol module (Mills et al., 2016) and has been extensively employed to investigate the impact of volcanic aerosols on heterogeneous processes and their impact on ozone loss (e.g., Mills et al., 2017; Stone et al., 2017; Zambri et al., 2019). The reaction probabilities for key stratospheric heterogeneous processes on sulfate aerosol used in WACCM are listed in Table S1.

For this study, the simulations are characterized by a horizontal resolution of 0.9° latitude × 1.25° longitude, utilizing the finite volume dynamical core (Lin & Rood, 1996). The model includes 110 vertical levels, with a vertical resolution of approximately 500m in the upper troposphere and lower stratosphere. WACCM6 is operated in a specified dynamics configuration, where temperatures and horizontal winds (U, V) are relaxed, or nudged, to the Modern-Era Retrospective analysis for Research and Applications Version 2 (MERRA-2) reanalysis (Gelaro et al., 2017) using a relaxation timescale of 12 hours. The nudging method employed in this study follows the approach outlined by Davis et al. (2022). This configuration spans from 2007 until the end of 2022, initialized with conditions from a long historical simulation (Gettelman et al., 2019). The model setup incorporates major stratospheric volcanic injections from 2007 to 2021. Beginning in January 2022, two distinct cases are conducted: the volcano case with external forcing (SO_2 and H_2O injection) from the HTHH eruption, and the control case with no external forcing (no SO_2 nor H_2O injection) from the HTHH eruption. The disparity between these two nudged simulations provides insights into the chemistry-related changes post the HTHH eruption. This study assumes the emissions are 150 Tg H_2O and 0.6 Tg SO_2 on January 15, 2022, from approximately 20 to 35 km altitude. The injection profiles of H_2O and SO_2 are similar to Zhu et al. (2022), however, with an adjustment of SO_2 injection. The SO_2 injection estimate ranges from 0.4 Tg to 1 Tg (e.g., Millan et al., 2022; Li et al., 2023; Sellitto et al., 2023) from different sources and approaches. Here an SO_2 injection of 0.6 Tg is utilized, leading to aerosol extinction that exhibits strong agreement with the Ozone Mapping and Profiler Suite Limb Profiler (OMPS-LP) observation, especially during the 2022 Austral winter (Figure S1).

2.3 Tracer-tracer method

Exploring the correlation among chemical species, commonly known as "tracer–tracer" analysis, serves as a robust approach to dissect the interactions between dynamical and chemical processes (e.g., Proffitt et al., 1990; Griffin et al., 2019). In this study, we construct a “no-chemistry” baseline from the linear fit between N_2O and HCl over January to March data, since no or little heterogeneous chemistry normally occurs in these three months given warm conditions. The foundation of this analysis lies in the expectation that dynamical transport should impact both N_2O and HCl in a similar manner. The deviations of HCl from this “no-chemistry” baseline are defined as ΔHCl, indicating the changes in HCl that are due to chemical processes. A detailed discussion on this method can be found in Wang et al., (2023).

In this analysis, N_2O serves as an inactive tracer for calculating ΔHCl, given its availability in both ACE and MLS observations. The distinct long-term trends of N_2O and HCl resulting from anthropogenic emissions could introduce a bias in the tracer-tracer correlation. Furthermore, the drifting issue associated with MLS N_2O adds complexity to the long-term trends. To address this, ΔHCl for each year is computed based on the "no-chemistry" baseline established in that specific year. This approach prevents long-term trends in N_2O and HCl from affecting the calculations.

3. Results and Discussions

3.1 Chemical signal of HCl loss at mid-latitudes (30-55°S)

The 2022 anomalies are computed as deviations from the climatological mean, shown in Figure 1. We linearly detrend both satellite observations and model simulations using data from 2007 to 2019 to accommodate the long-term trends in N_2O and HCl as well as additional instrumental drift in MLS N_2O. The climatology encompasses various phases of the Quasi-Biennial Oscillation (QBO). Therefore, the derived stratospheric anomalies in HCl and N_2O reflect both the influence of the 2022 QBO phase and the forced changes after the HTHH eruption, including both dynamical and chemical impacts. We use N_2O, a long-lived transport tracer, to clarify the influence of dynamics in shaping the distribution of trace gasses. Notably, in much of the lower stratosphere, the vertical and meridional gradients of N_2O exhibit an opposite pattern to HCl. As a result, N_2O is generally anticorrelated with HCl in the lower stratosphere. The hatched regions on the plot denote areas where the 2022 anomalies fall outside the range of all variability during the period 2007-2019. Specifically, for N_2O and HCl, the hatches indicate that the 2022 value represents the maximum and minimum, respectively, compared to the climatological data. The WACCM N_2O anomaly is consistent with observations, suggesting that the dynamical transport on tracer distribution is represented well in WACCM.

The WACCM HCl anomaly in 2022 closely aligns with ACE and MLS relative to the climatology. These anomalies arise from a combination of internal variability and the forced dynamical and chemical changes triggered by the HTHH eruption. The onset of the negative anomaly in HCl is evident from May, corresponding to the arrival of substantial aerosols from the HTHH eruption in this region (Santee et al., 2023). During the months of June, July, and August (JJA), ACE, MLS, and WACCM consistently depict the lowest HCl levels compared to all years included in the climatology (indicated by hatching in Figure 1), consistent with the large negative HCl anomaly in winter reported in Wilmouth et al., (2023). In the latter part of the year, specifically between 17 to 27 km, both model and observations exhibit a substantial negative anomaly in HCl. Despite the

potential for chemical processing in this region, the signal of such processing is largely overshadowed by significant countervailing positive anomalies in N_2O, indicating the predominant influence of transport effects. However, in the key altitude range of approximately 19 to 23 km during JJA that we focus on here, the large HCl anomaly is not accompanied by a similarly large N_2O anomaly. This discrepancy suggests that dynamics alone cannot account for the low HCl levels in that region, and chemical processing is highly likely taking place. The subsequent analysis will focus on this specific region during the SH winter months.

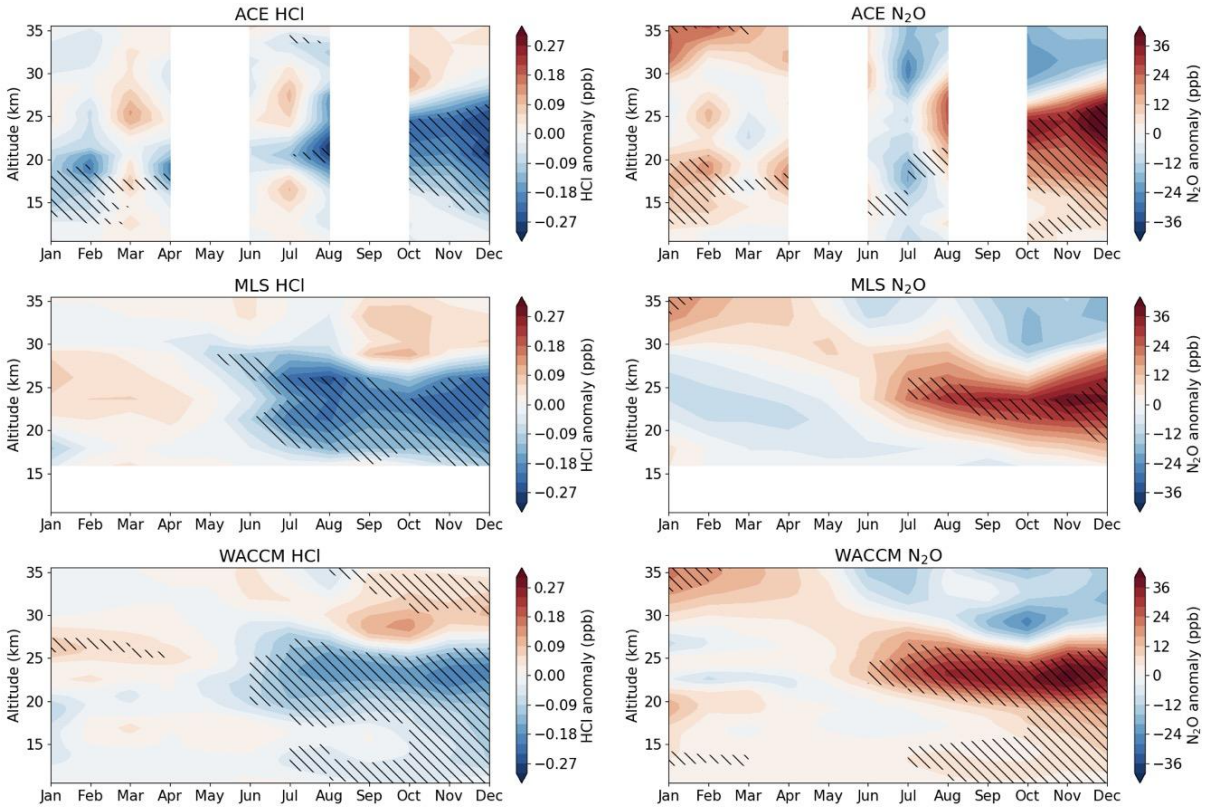

Figure 1. Calculated 2022 HCl anomaly in ppbv (left panels) and N_2O anomaly in ppbv (right panels) relative to climatology (2007 to 2019) from ACE, MLS, and WACCM in the SH mid-latitudes (30-55°S). Hatched regions indicate where the 2022 anomalies are outside the range of all variability during 2007-2019.

3.2 Significant stratospheric chlorine activation

The top panel in Figure 2 depicts the tracer-tracer relationship of ACE N_2O and HCl in June, July, August and October at 20.5 km over 30 to 55°S, color-coded by water vapor concentration. ACE doesn't have observations in May and September 2022 over this latitude range. The thick black lines in the top panel of Figure 2 represent the "no-chemistry" baseline in 2022, and the shaded area encompasses a conservative full range of baseline variability, bounded by the maximum and minimum baselines between 2007 and 2019. Deviations from correlation observed in HCl suggest the presence of chemical processes, as described in Wang et al. (2023). The intensity of chemical processes becomes more pronounced with greater deviations of HCl from the baseline. Tracer-tracer plots further confirm the strong chemical processing that occurs in June and intensifies in

July and August in 2022 compared to 2007 to 2019 (triangles in Figure 2). It is notable that deviations in HCl from their respective "no-chemistry" baseline occur in June to August from 2007 to 2019 (round points in Figure 2), as chlorine activation happens every year in these months with a seasonal cycle. In October, Cl activation slows down as the polar spring advances with temperature rise, thus the HCl departure from the baseline reduces.

The bottom panel of Figure 2 displays the derived ΔHCl resulting from chemical processes from MLS, ACE, and WACCM in 2022. ACE and MLS ΔHCl is calculated by the deviations from the baseline, with the seasonal cycle removed. The shaded regions in blue and red represent the range of ±1 standard deviation (std) for MLS and ACE, respectively, for each month from 2007 to 2019. The patterns of derived ΔHCl from observations closely resemble those calculated by WACCM from the two nudged simulations (volcano minus control). Notably, the largest chemical induced HCl reduction occurs in the SH winter. Figure 2 further indicates that tracer-tracer analysis can effectively be employed to derive ΔHCl due to chemical processes using MLS and ACE data, and the results exhibit comparability with those from the chemistry climate model. The differences between WACCM, ACE and MLS are within the uncertainty range (±1 std).

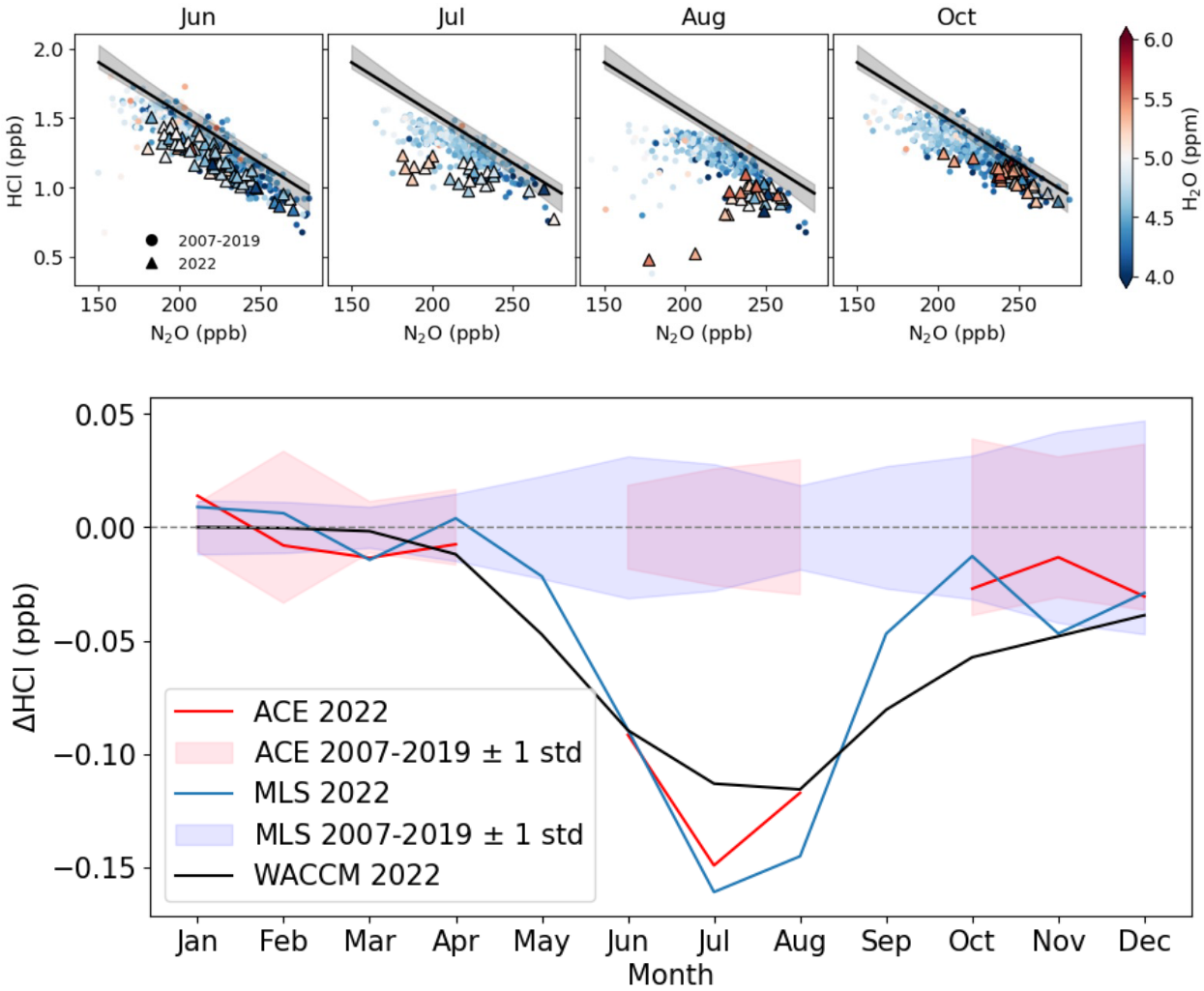

Figure 2. Top panel: Tracer–tracer correlation between ACE-measured N_2O (x-axis) and HCl (y-axis), color-coded by water vapor concentration. Each dot represents a single measurement at 20.5 km over 30 to 55°S. The thick black lines represent the no-chemistry baseline, from the linear fit over January to March 2022 data points. The shaded regions indicate a conservative full range of baseline variability bounded by the maximum and minimum baselines constructed by data in individual years from 2007 to 2019. Bottom panel: Calculated ΔHCl from ACE, MLS and WACCM in 2022 averaging all points over 30 to 55°S. ACE and MLS ΔHCl is calculated from departures from the baseline in the top panel but with the seasonal cycle removed, representing the change in HCl due to anomalous chemical processes in 2022. The blue and red shaded regions indicate ±1 standard deviation range for MLS and ACE in each month from 2007 to 2019. WACCM ΔHCl is calculated from the difference in HCl between the volcano and the control run.

3.3 Role of gas and heterogenous phase chemistry in chlorine activation

To understand the chemical processes that give rise to the ΔHCl in Figure 2 following the HTHH eruption, a thorough model examination is conducted. Figure 3 illustrates the changes in gas-phase

and heterogeneous-phase chemistry, along with the cumulative changes of all chemistry. The ΔHCl is calculated from the volcano case compared to the control case. Gas-phase chemistry (Figure 3a) results in an increase in HCl below 23 km over the 30 to 55°S, accompanied by a decrease from 23 to 30 km. Heterogeneous chemistry (Figure 3b) induces HCl depletion from 15 to 25 km. Considering both gas and heterogeneous chemistry (Figure 3c), the ΔHCl exhibits a net reduction above 19 km from April to December, with the maximum reduction occurring in the winter, consistent with Figure 2. There is an HCl increase below 18 km (Figure 3c), attributable to enhanced gas-phase reactions, particularly Cl+CH_4 and ClO+OH (discussed below).

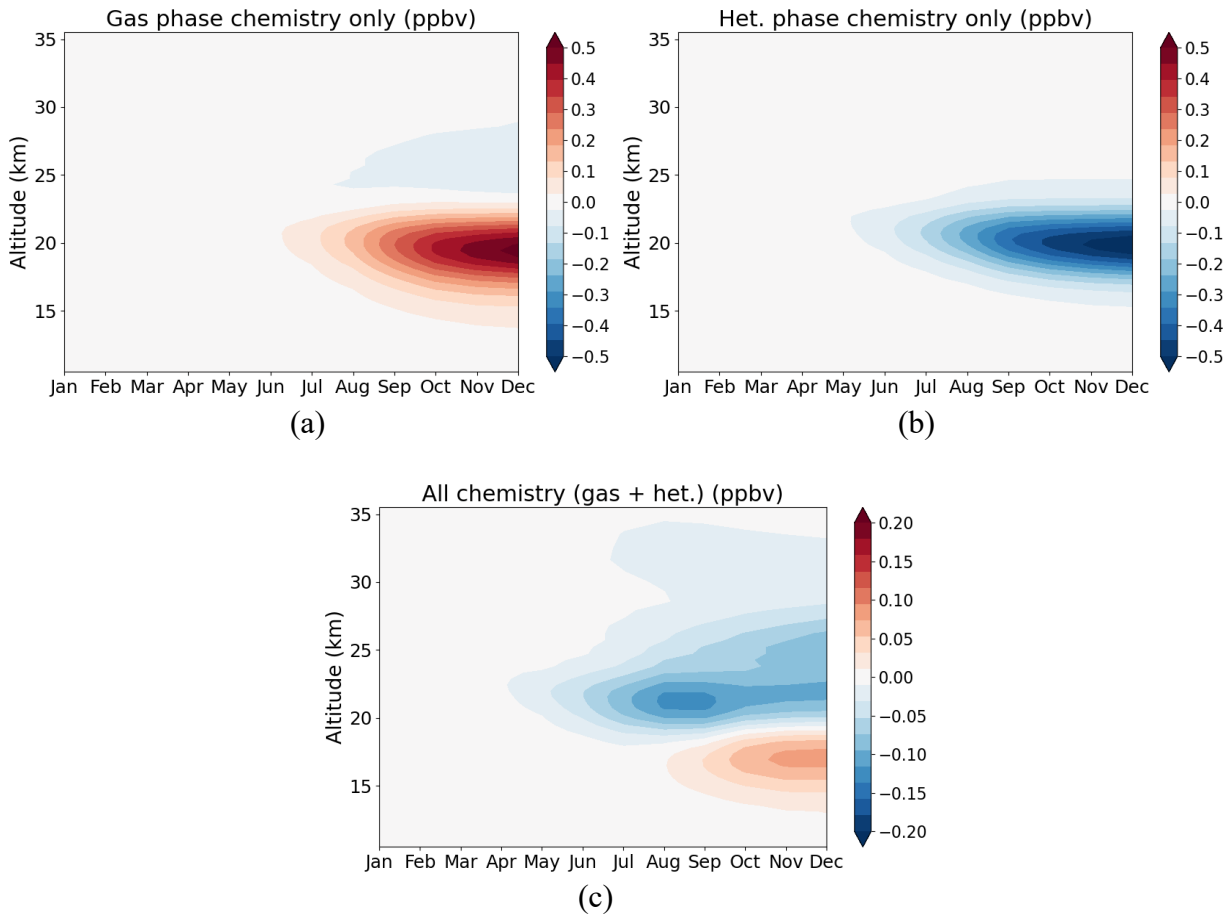

Figure 3. WACCM calculated ΔHCl (ppbv) from the volcano minus the control case for (a) gas-phase chemistry only, (b) heterogeneous chemistry only and (c) the sum of all gas and heterogeneous chemistry over 30 to 55°S. Note that panels c has different color bar ranges from panels a and b.

Perturbations in individual reactions are investigated following the HTHH eruption, with a particular focus during JJA. The ones with important contributions to the ΔHCl are plotted in Figure 4 with different colors. The rest of the reactions only affect less than 1% of ΔHCl, thus are not shown here. A full list of HCl reactions examined can be found in Table S2. The "all gas" black line in Figure 4a adds up all the gas reactions, not just the gas terms plotted in the figures, and same for the "all het" black line in Figure 4b. In the realm of gas-phase chemistry (Figure 4a), the reaction between HCl and elevated OH acts as a significant sink for HCl from the simulated

perturbation due to HTHH. However, this loss is entirely compensated for by the heightened gas-phase production, particularly $Cl+CH_4$ and ClO+OH. Among heterogeneous reactions (Figure 4b), the primary sink for HCl is the reaction between HOBr and HCl on sulfate aerosols between 15 to 25 km, with $ClONO_2$+HCl contributing as well, albeit with a much smaller magnitude. This is mainly attributed to volcanic aerosols providing additional surface area density (SAD) for heterogeneous chemistry at these altitudes (Figure 4d). Here we conclude that, during the SH wintertime, the HCl chemical reduction from 15 to 24 km in the mid-latitudes is attributed to heterogeneous chemistry rather than gas-phase chemistry (Figure 4c). Our results for this season differ from the findings reported by Wilmouth et al. (2023), where they suggest that gas-phase chemistry is the primary cause of the chemical loss of HCl. They state that this is because of the enhanced HCl loss with elevated OH, as well as the slower HCl production from $Cl+CH_4$ reaction. Our findings support the former but not the latter, resulting in a different net effect for gas-phase reactions alone.

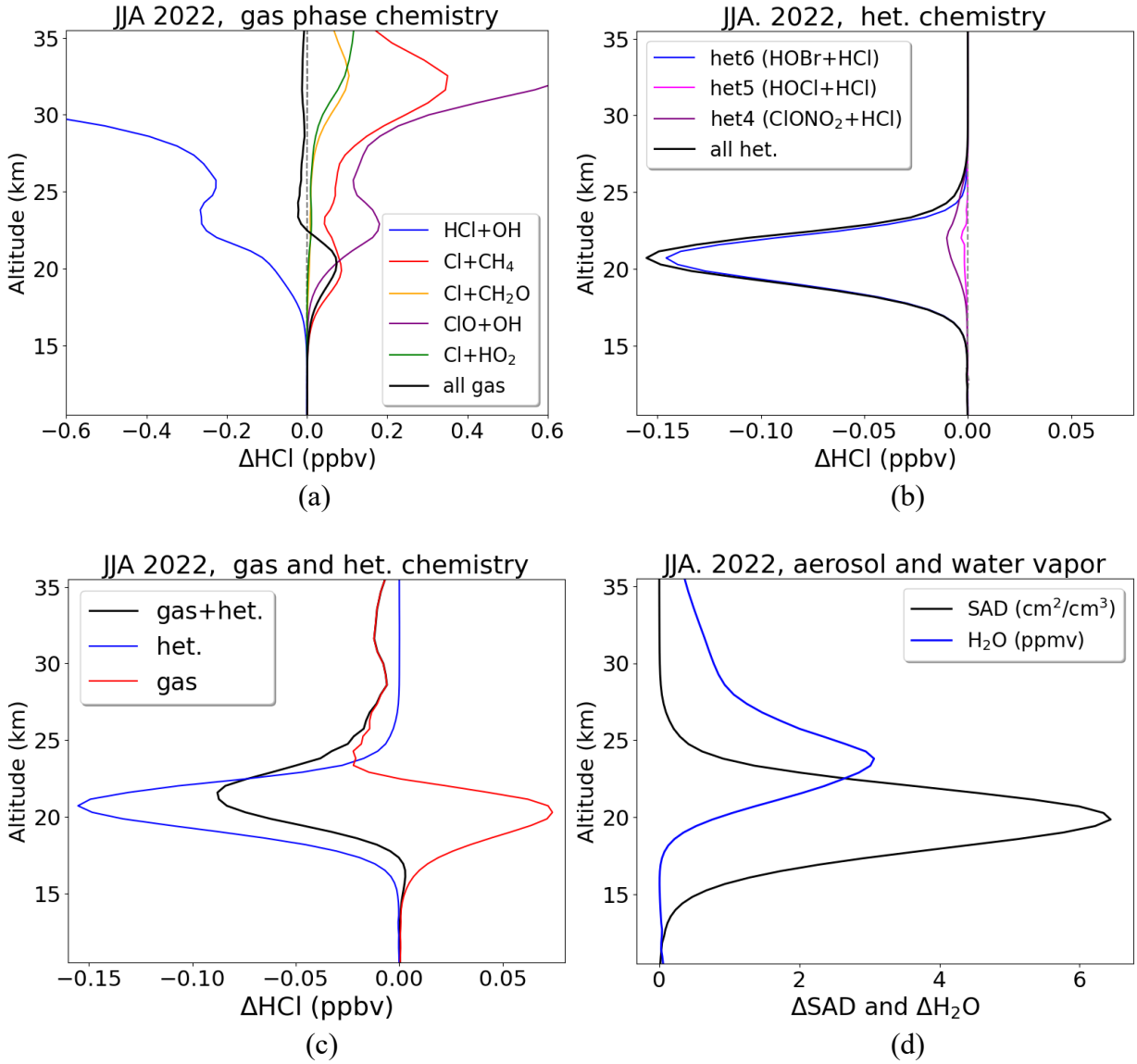

Figure 4. ΔHCl (in ppbv) contribution from individual reactions for (a) gas chemistry, (b) heterogeneous chemistry and (c) the sum of all chemistry averaged over JJA in 2022 over 30 to 55°S. ΔHCl is calculated from the volcano minus control case. (d) the modeled aerosol surface area density in um^2/cm^3 and water in ppmv.

The injection of volcanic water and aerosols from the HTHH eruption perturbs atmospheric conditions (e.g., surface area density, aerosol radiance and H_2SO_4 content), which further impact the reactive probability of heterogeneous reactions. Comparative analysis between the volcano case and the control case reveals enhanced reactive probabilities for all examined heterogeneous reactions in the volcano scenario (Figure S2). Laboratory studies (Hanson and Ravishankara, 1995; Hanson et al., 1996, 2003) have demonstrated the highly efficient hydrolysis of $BrONO_2$ in sulfuric acid solutions. Reaction probabilities of approximately 0.8 were documented for the uptake of $BrONO_2$ onto sulfuric acid solutions with H_2SO_4 content ranging from 40 to 70 weight percentage (wt%) (Figure S2). The enhanced water concentration at mid-latitudes doesn't substantially decrease the sulfuric acid content during the SH winter, unlike immediately after the eruption when the massive influx of water reduces the weight percent of H_2SO_4 from 70% to 35% (Zhu et al., 2023). Compared to other heterogeneous processes, hydrolysis of $BrONO_2$ is relatively temperature-insensitive and can take place rapidly at various stratospheric conditions, making their influence important and widespread. The product resulting from the hydrolysis of $BrONO_2$, HOBr, undergoes another heterogeneous process with HCl, providing an additional pathway to chlorine activation. Under temperatures in the mid-latitudes (>200K), the enhancement in the rate of HOBr+HCl reactions after the HTHH eruption plays a dominant role in HCl depletion among all the heterogeneous processes.

4. Summary and discussion

In summary, we have examined the mid-latitudes HCl reduction in the SH winter following the eruption of HTHH using satellite data and global chemistry-climate model. Our analysis indicates a significant role for heterogeneous chemical processing in the observed HCl reduction. The results confirm that the tracer-tracer method provides a good estimate of the chemical impacts distinct from dynamics. And the derived chemical HCl change is consistent among ACE, MLS and WACCM. Further delving into WACCM's detailed chemistry, we examine individual chlorine gas-phase and heterogeneous reactions. We find that despite a substantial increase in the reaction of HCl with elevated OH in the SH winter, this loss is entirely compensated for by heightened gas-phase production from $Cl+CH_4$ and ClO+OH. Heterogeneous chemistry emerges as the primary driver for the chemical loss of HCl, with the reaction between HOBr and HCl on sulfate aerosols identified as the most crucial process. Our study provides useful information for understanding volcanic impacts on stratospheric chemistry, particularly their detailed breakdown among gas-phase and heterogeneous reactions at mid-latitudes.

Acknowledgments

Jun Zhang is supported by the NSF via NCAR's Advanced Study Program Postdoctoral Fellowship. Douglas Kinnison is partially supported by NASA grant no. 80NSSC19K0952. Peidong Wang, Susan Solomon and Jian Guan gratefully acknowledge support by NSF-AGS [2316980]. NCAR's Community Earth System Model project is supported primarily by the National Science Foundation. This material is based upon work supported by the NSF National Center for Atmospheric Research, which is a major facility sponsored by the U.S. National Science Foundation under Cooperative Agreement No. 1852977. Computing and data storage resources, including the Cheyenne supercomputer (doi:10.5065/D6RX99HX), were provided by the Computational and Information Systems Laboratory (CISL) at NCAR. This project received

funding from NOAA's Earth Radiation Budget (ERB) Initiative (CPO #03-01-07-001). Yunqian Zhu is supported in part by NOAA cooperative agreements NA17OAR4320101 and NA22OAR4320151.

Open Research

CESM2/WACCM6 (described in Gettelman et al., 2019) is an open-source community model, which was developed with support primarily from the National Science Foundation. Figures in this study are plotted using an open-source software Python. The atmospheric modeling dataset used in the analysis is published (Zhang et al., 2024).

References

Abbatt, J. P. (1995). Interactions of HBr, HCl, and HOBr with supercooled sulfuric acid solutions of stratospheric composition. *Journal of Geophysical Research: Atmospheres*, 100(D7), 14009-14017.

Anderson, J. G., Wilmouth, D. M., Smith, J. B., & Sayres, D. S. (2012). UV dosage levels in summer: Increased risk of ozone loss from convectively injected water vapor. *Science*, 337(6096), 835-839.

Bernath, P., Boone, C., & Crouse, J. (2022). Wildfire smoke destroys stratospheric ozone. *Science*, 375(6586), 1292-1295.

Carn, S. A., Krotkov, N. A., Fisher, B. L., & Li, C. (2022). Out of the blue: Volcanic SO2 emissions during the 2021–2022 eruptions of Hunga Tonga—Hunga Ha'apai (Tonga). *Frontiers in Earth Science*, 10, 976962. https://doi.org/10.3389/feart.2022.976962

Davis, N. A., Callaghan, P., Simpson, I. R., & Tilmes, S. (2022). Specified dynamics scheme impacts on wave-mean flow dynamics, convection, and tracer transport in CESM2 (WACCM6). *Atmospheric Chemistry and Physics*, 22(1), 197-214. https://doi.org/10.5194/acp-22-197-2022

Gelaro, R., McCarty, W., Suárez, M. J., Todling, R., Molod, A., Takacs, L., ... & Zhao, B. (2017). The modern-era retrospective analysis for research and applications, version 2 (MERRA-2). *Journal of climate*, 30(14), 5419-5454. https://doi.org/10.1175/JCLI-D-16-0758.1

Gettelman, A., Mills, M. J., Kinnison, D. E., Garcia, R. R., Smith, A. K., Marsh, D. R., ... & Randel, W. J. (2019). The whole atmosphere community climate model version 6 (WACCM6). *Journal of Geophysical Research: Atmospheres*, 124(23), 12380-12403. https://doi.org/10.1029/2019JD030943

Griffin, D., Walker, K. A., Wohltmann, I., Dhomse, S. S., Rex, M., Chipperfield, M. P., ... & Tarasick, D. (2019). Stratospheric ozone loss in the Arctic winters between 2005 and 2013 derived with ACE-FTS measurements. *Atmospheric Chemistry and Physics*, 19(1), 577-601.

Mills, M. J., Kinnison, D. E., Garcia, R. R., Smith, A. K., Marsh, D. R., ... & Randel, W. J. (2019). The whole atmosphere community climate model version 6 (WACCM6). *Journal of Geophysical Research: Atmospheres*, 124(23), 12380-12403. https://doi.org/10.1029/2019JD030943

Hanson, D. R., Ravishankara, A. R., & Solomon, S. (1994). Heterogeneous reactions in sulfuric acid aerosols: A framework for model calculations. *Journal of Geophysical Research: Atmospheres*, 99(D2), 3615-3629.

Hanson, D. R., & Ravishankara, A. R. (1995). Heterogeneous chemistry of bromine species in sulfuric acid under stratospheric conditions. *Geophysical research letters*, 22(4), 385-388.

Hanson, D. R., Ravishankara, A. R., & Lovejoy, E. R. (1996). Reaction of BrONO2 with H2O on submicron sulfuric acid aerosol and the implications for the lower stratosphere. *Journal of Geophysical Research: Atmospheres*, 101(D4), 9063-9069.

Hanson, D. R. (2003). Reactivity of BrONO2 and HOBr on sulfuric acid solutions at low temperatures. *Journal of Geophysical Research: Atmospheres*, 108(D8).

Hofmann, D. J., & Solomon, S. (1989). Ozone destruction through heterogeneous chemistry following the eruption of El Chichon. *Journal of Geophysical Research: Atmospheres*, 94(D4), 5029-5041. https://doi.org/10.1029/JD094iD04p05029

Kawa, S. R., Newman, P. A., Lait, L. R., Schoeberl, M. R., Stimpfle, R. M., Kohn, D. W., ... & Loewenstein, M. (1997). Activation of chlorine in sulfate aerosol as inferred from aircraft observations. *Journal of Geophysical Research: Atmospheres*, 102(D3), 3921-3933.

Li, Z., Bi, J., Hu, Z., Ma, J., & Li, B. (2023). Regional transportation and influence of atmospheric aerosols triggered by Tonga volcanic eruption. *Environmental Pollution*, 325, 121429.

Lin, S. J., & Rood, R. B. (1996). Multidimensional flux-form semi-Lagrangian transport schemes. *Monthly Weather Review*, 124(9), 2046-2070. https://doi.org/10.1175/1520-0493(1996)124<2046:MFFSLT>2.0.CO;2

Livesey, N J, W G Read, P A Wagner, L Froidevaux, M L Santee, and M J Schwartz. 2020. "Version 5.0 x Level 2 and 3 Data Quality and Description Document (Tech. Rep. No. JPL D-105336 Rev. A)." *Jet Propulsion Laboratory*.

Livesey, N. J., Read, W. G., Froidevaux, L., Lambert, A., Santee, M. L., Schwartz, M. J., ... & Nedoluha, G. E. (2021). Investigation and amelioration of long-term instrumental drifts in water vapor and nitrous oxide measurements from the Aura Microwave Limb Sounder (MLS) and their implications for studies of variability and trends. *Atmospheric Chemistry and Physics*, 21(20), 15409-15430.

Millan, L., Santee, M. L., Lambert, A., Livesey, N. J., Werner, F., Schwartz, M. J., ... & Froidevaux, L. (2022). The Hunga Tonga-Hunga Ha'apai hydration of the stratosphere. *Geophysical Research Letters*, 49(13), e2022GL099381. https://doi.org/10.1029/2022GL099381

Mills, M. J., Schmidt, A., Easter, R., Solomon, S., Kinnison, D. E., Ghan, S. J., ... & Gettelman, A. (2016). Global volcanic aerosol properties derived from emissions, 1990–2014, using CESM1 (WACCM). *Journal of Geophysical Research: Atmospheres*, 121(5), 2332-2348. https://doi.org/10.1002/2015JD024290

Mills, M. J., Richter, J. H., Tilmes, S., Kravitz, B., MacMartin, D. G., Glanville, A. A., ... & Kinnison, D. E. (2017). Radiative and chemical response to interactive stratospheric sulfate aerosols in fully coupled CESM1 (WACCM). *Journal of Geophysical Research: Atmospheres*, 122(23), 13-061. https://doi.org/10.1002/2017JD027006

Proffitt, M. H., Margitan, J. J., Kelly, K. K., Loewenstein, M., Podolske, J. R., & Chan, K. R. (1990). Ozone loss in the Arctic polar vortex inferred from high-altitude aircraft measurements. *Nature*, 347(6288), 31-36.

Randel, W. J., Johnston, B. R., Braun, J. J., Sokolovskiy, S., Vömel, H., Podglajen, A., & Legras, B. (2023). Stratospheric Water Vapor from the Hunga Tonga–Hunga Ha'apai Volcanic Eruption Deduced from COSMIC-2 Radio Occultation. *Remote Sensing*, 15(8), 2167. https://doi.org/10.3390/rs15082167

Santee, M. L., Lambert, A., Froidevaux, L., Manney, G. L., Schwartz, M. J., Millán, L. F., et al. (2023). Strong evidence of heterogeneous processing on stratospheric sulfate aerosol in the extrapolar Southern Hemisphere following the 2022 Hunga Tonga-Hunga Ha'apai eruption. *Journal of Geophysical Research: Atmospheres*, 128, e2023JD039169. https://doi.org/10.1029/2023JD039169

Sellitto, P., Siddans, R., Belhadji, R., Carboni, E., Legras, B., Podglajen, A., ... & Kerridge, B. (2023). Observing the SO2 and Sulphate Aerosol Plumes from the 2022 Hunga Tonga-Hunga Ha'apai Eruption with IASI. *Authorea Preprints*.

Shi, Q., Jayne, J. T., Kolb, C. E., Worsnop, D. R., & Davidovits, P. (2001). Kinetic model for reaction of ClONO2 with H2O and HCl and HOCl with HCl in sulfuric acid solutions. *Journal of Geophysical Research: Atmospheres,* 106(D20), 24259-24274.

Slusser, J. R., Fish, D. J., Strong, E. K., Jones, R. L., Roscoe, H. K., & Sarkissian, A. (1997). Five years of NO2 vertical column measurements at Faraday (65 S): Evidence for the hydrolysis of BrONO2 on Pinatubo aerosols. *Journal of Geophysical Research: Atmospheres*, 102(D11), 12987-12993.

Solomon, S., Garcia, R. R., Rowland, F. S., & Wuebbles, D. J. (1986). On the depletion of Antarctic ozone. *Nature*, 321(6072), 755-758.

Solomon, S. (1999). Stratospheric ozone depletion: A review of concepts and history. *Reviews of geophysics*, 37(3), 275-316. https://doi.org/10.1029/1999RG900008

Solomon, S., Kinnison, D., Bandoro, J., & Garcia, R. (2015). Simulation of polar ozone depletion: An update. *Journal of Geophysical Research: Atmospheres*, 120(15), 7958-7974. https://doi.org/10.1002/2015JD023365

Solomon, S., Stone, K., Yu, P., Murphy, D. M., Kinnison, D., Ravishankara, A. R., & Wang, P. (2023). Chlorine activation and enhanced ozone depletion induced by wildfire aerosol. Nature, 615(7951), 259-264.

Stone, K. A., Solomon, S., Kinnison, D. E., Pitts, M. C., Poole, L. R., Mills, M. J., ... & Hagiya, S. (2017). Observing the impact of Calbuco volcanic aerosols on South Polar ozone depletion in 2015. *Journal of Geophysical Research: Atmospheres*, 122(21), 11-862. https://doi.org/10.1002/2017JD026987

Taha, G., Loughman, R., Colarco, P. R., Zhu, T., Thomason, L. W., & Jaross, G. (2022). Tracking the 2022 Hunga Tonga-Hunga Ha'apai aerosol cloud in the upper and middle stratosphere using space-based observations. *Geophysical Research Letters*, 49(19), e2022GL100091. https://doi.org/10.1029/2022GL100091

Tie, X., & Brasseur, G. (1996). The importance of heterogeneous bromine chemistry in the lower stratosphere. *Geophysical research letters*, 23(18), 2505-2508.

Wang, P., Solomon, S., & Stone, K. (2023). Stratospheric chlorine processing after the 2020 Australian wildfires derived from satellite data. *Proceedings of the National Academy of Sciences*, 120(11), e2213910120.

Wang, X., Randel, W., Zhu, Y., Tilmes, S., Starr, J., Yu, W., ... & Li, J. (2023). Stratospheric Climate Anomalies and Ozone Loss Caused by the Hunga Tonga-Hunga Ha'apai Volcanic Eruption. *Journal of Geophysical Research: Atmospheres*, 128(22), e2023JD039480. https://doi.org/10.1029/2023JD039480

Waschewsky, G. C., & Abbatt, J. P. (1999). HOBr in sulfuric acid solutions: Solubility and reaction with HCl as a function of temperature and concentration. *The Journal of Physical Chemistry A*, 103(27), 5312-5320.

Wilmouth, D. M., Østerstrøm, F. F., Smith, J. B., Anderson, J. G., & Salawitch, R. J. (2023). Impact of the Hunga Tonga volcanic eruption on stratospheric composition. *Proceedings of the National Academy of Sciences*, 120(46), e2301994120.

Zambri, B., Solomon, S., Kinnison, D. E., Mills, M. J., Schmidt, A., Neely III, R. R., ... & Roth, C. Z. (2019). Modeled and observed volcanic aerosol control on stratospheric NOy and Cly. *Journal of Geophysical Research: Atmospheres*, 124(17-18), 10283-10303. https://doi.org/10.1029/2019JD031111

Zhang, J., Kinnison, D. E., Zhu, Y., Wang, X., Tilmes, S., Dubé, K. R., & Randel, W. J. (2023). Chemistry contribution to stratospheric ozone depletion after the unprecedented water rich Hunga Tonga eruption. *Authorea Preprints*.

Zhang, J., Kinnison, D., Zhu, Y., Wang, X., Tilmes, S., Dube, K., Randel, W., (Version 1.0.) [Dataset] (2023). UCAR/NCAR - GDEX. https://doi.org/10.5065/nsar-fh76

Zhang, J., Wang, P., Kinnison, D., Solomon, S., Guan, J., Zhu, Y., (Version 1.0.) [Dataset] (2024). UCAR/NCAR - GDEX. https://doi.org/10.5065/j6yg-a009

Zhu, Y., Bardeen, C. G., Tilmes, S., Mills, M. J., Wang, X., Harvey, V. L., ... & Toon, O. B. (2022). Perturbations in stratospheric aerosol evolution due to the water-rich plume of the 2022 Hunga-Tonga eruption. *Communications Earth & Environment*, 3(1), 248. https://doi.org/10.1038/s43247-022-00580-w

Zhu, Y., Portmann, R. W., Kinnison, D., Toon, O. B., Millán, L., Zhang, J., ... & Rosenlof, K. H. (2023). Stratospheric ozone depletion inside the volcanic plume shortly after the 2022 Hunga Tonga eruption. *Atmospheric Chemistry and Physics*, 23(20), 13355-13367.

Geophysical Research Letters

Supporting Information for

Stratospheric chlorine processing after the unprecedented Hunga Tonga eruption

Authors: Jun Zhang[1*], Peidong Wang[2], Douglas Kinnison[1], Susan Solomon[2], Jian Guan[2], Yunqian Zhu[3,4]

Affiliations:

[1]Atmospheric Chemistry Observations & Modeling Laboratory, NSF National Center for Atmospheric Research, Boulder, CO, USA

[2] Department of Earth, Atmospheric, and Planetary Sciences, Massachusetts Institute of Technology, Cambridge, MA, USA, 02139

[3] Cooperative Institute for Research in Environmental Sciences, University of Colorado Boulder, Boulder, CO, USA, 80309

[4]Chemical Sciences Laboratory, National Oceanic and Atmospheric Administration, Boulder, CO, USA, 80305

[*]Corresponding author: Jun Zhang (jzhan166@ucar.edu)

Contents of this file

Introduction

Supporting information includes text and figures to support the discussion in the main article.

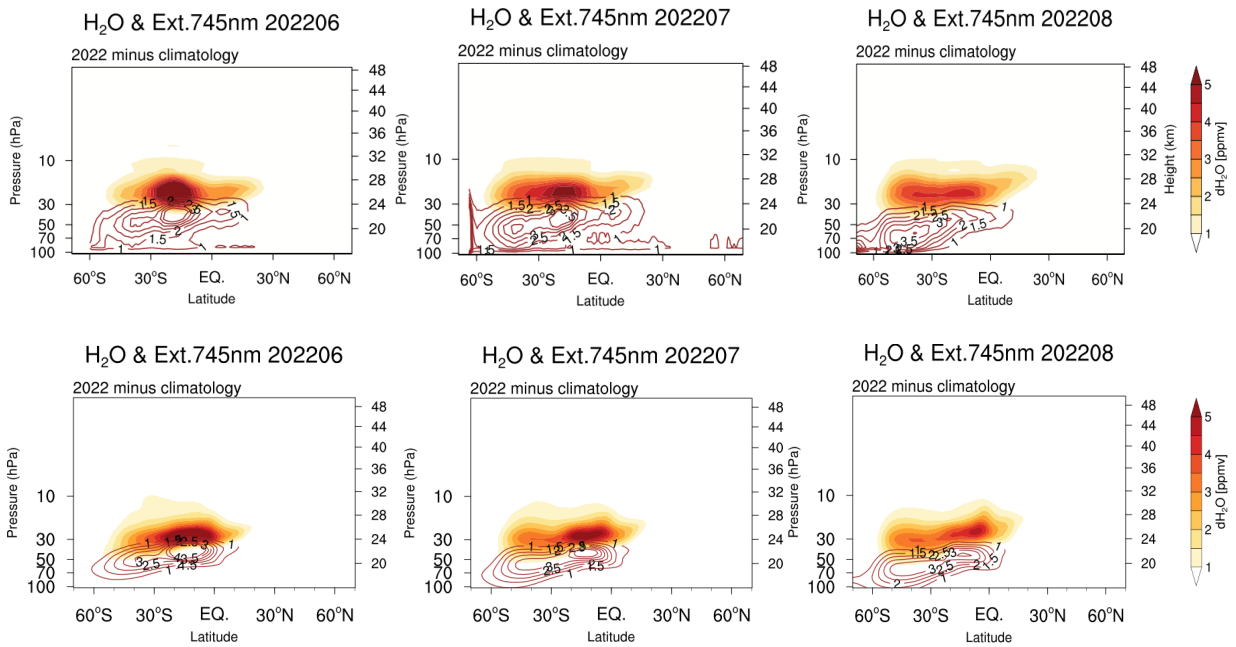

Figure S1. Observed and simulated H_2O and aerosol perturbations after the HTHH eruption in JJA 2022. Top: observed H_2O from MLS overlayed with OMPS aerosol extinction. Bottom: WACCM simulated H_2O and aerosol extinction.

Table S1. Heterogeneous Reaction Probabilities for sulfate aerosol used in WACCM.

Reactions	Reaction probability
$HCl + ClONO_2 \rightarrow Cl_2 + HNO_3$	Shi et al. (2001)
$ClONO_2 + H_2O \rightarrow HOCl + HNO_3$	Shi et al. (2001)
$BrONO_2 + H_2O \rightarrow HOBr + HNO_3$	Hanson et al. (1996)
$HOCl + HCl \rightarrow Cl_2 + H_2O$	Shi et al. (2001)
$HOBr + HCl \rightarrow BrCl + H_2O$	Hanson (2003)

Table S2. Full list of HCl reactions examined in this study.

Gas-phase production:

$Cl + CH_2O \rightarrow HCl + HO_2 + CO$

$Cl + CH_4 \rightarrow CH_3O_2 + HCl$

$Cl + H_2 \rightarrow HCl + H$

$Cl + H_2O_2 \rightarrow HCl + HO_2$

$Cl + HO_2 \rightarrow HCl + O_2$

$ClO + OH \rightarrow HCl + O_2$

$HOCl + Cl \rightarrow HCl + ClO$

$CH_2Br_2 + Cl \rightarrow 2*Br + HCl$

$CH_3Br + Cl \rightarrow HCl + HO_2 + Br$

$CH_3Cl + Cl \rightarrow HO_2 + CO + 2*HCl$

$CHBr_3 + Cl \rightarrow 3*Br + HCl$

$C_2H_6 + Cl \rightarrow HCl + C_2H_5O_2$

Gas-phase loss:

$HCl + hv \rightarrow H + Cl$

$HCl + O \rightarrow Cl + OH$

$HCl + OH \rightarrow H_2O + Cl$

$O1D + HCl \rightarrow Cl + OH$

$O1D + HCl \rightarrow ClO + H$

Heterogeneous loss:

[het4] $ClONO_2 + HCl \rightarrow Cl_2 + HNO_3$

[het5] $HOCl + HCl \rightarrow Cl_2 + H_2O$

[het6] $HOBr + HCl \rightarrow BRCl + H_2O$

[het9] $ClONO_2 + HCl \rightarrow Cl_2 + HNO_3$

[het10] $HOCl + HCl \rightarrow Cl_2 + H_2O$

[het15] $ClONO_2 + HCl \rightarrow Cl_2 + HNO_3$

[het16] $HOCl + HCl \rightarrow Cl_2 + H_2O$

[het17] $HOBr + HCl \rightarrow BrCl + H_2O$

Het 4,5,6 are reactions on sulfate aerosol;

Het 9,10 are reactions on nitric acid trihydrate;

Het 15,16,17 are reactions on ice.

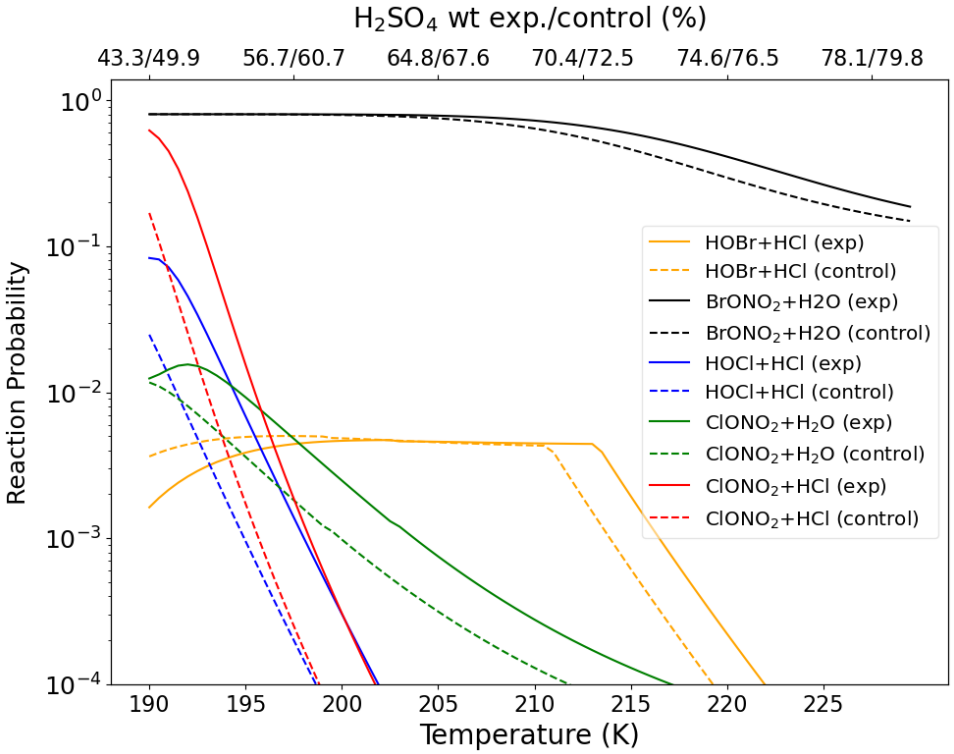

Figure S2. Reaction probability as a function of temperature for key stratospheric heterogeneous processes on sulfuric acid aerosols from the volcano (solid lines) and control (dashed lines) case in June 2022 at 40°S and 30 hPa. The H_2SO_4 wt.% is shown at the top of the graph for volcano and control case respectively.